Helium Migration in Iron

Y. Zhang
Christ's College

Department of Materials Science and Metallurgy
University of Cambridge

August 31, 2004

Preface

This dissertation is submitted for the Certificate of Post Graduate Studies in Natural Sciences at the University of Cambridge. The work reported was carried out under the supervision of Professor H. K. D. H. Bhadeshia and Mr. R. Kemp in the Department of Materials Science and Metallurgy between May 2004 and August 2004. To the best of my knowledge, this work is original, except where suitable references are made to previous work. Neither this, nor any substantially similar dissertation has been submitted for any degree, diploma or qualification at any other university or institution.

Y. Zhang
August 31, 2004

Acknowledgments

My deepest gratitude to my supervisor, Professor H.K.D.H. Bhadeshia for his constant guidance and encouragement, and for his unique way of teaching the simplicity and beauty of everything that surrounds us. I would also like to thank my demonstrator Mr R. Kemp who helped me with every detailed question.

I would like to thank all the people in the Phase Transformations and Com- plex Properties Research Group for all the happy time we shared and especially Mohammed who was there whenever I needed help with Latex.

I would like to thank all thirteen chevaliers of the M.Phil. class of 2003/2004 for their friendship and helps throughout the year.

I am extremely grateful my senior tutor in Christ's college Dr K. Bowkette for his valuable advice and financial assistance in this course.

I would also like to thank my family for their love and constant support without which I won't be able have the achievement at all.

Abstract

A theoretical model of helium migration in body centred cubic (BCC)structure irons has been developed using the concept of the effective helium diffusion coefficient with the method of rate theory equations. Various helium migration mechanisms have been identified under irradiation conditions. Comparison of the effects of BCC structure and FCC structure on the effective diffusion coefficient was also made to examine the possibility of the application of BCC irons in fusion reactors. The effects of both external parameters such as temperature, helium production rate, radiation damage rate and internal parameters such as cavities, grain sizes and dislocations on the diffusion mechanisms have been investigated. It is hoped the model can be validated with experimental data from fusion nuclear reactors available in the future and be used to examine the consequences of the diffusion on helium bubble growth and coalescence.

Contents

List of Figures

Nomenclature

ITER	International Thermonuclear Experimental Reactor
BCC	Body Centred Cubic
FCC	Face Centred Cubic
SIA	Self-interstitial atom
UTS	Ultimate tensile strengh (MPa)
k	Boltzmann's constant
T	Temperature (K)
t	Time (s)
D_{He}^{M}	Helium diffusion coefficient (cm^2s^{-1})
D_{He}^{eff}	Effective migration diffusion coefficient (cm^2s^{-1})
D_{01}	Diffusion coefficient of helium interstitial atoms (cm^2s^{-1})
D_{11}	Diffusion coefficient of helium substitutional atoms (cm^2s^{-1})
σ	Atomic volume ($Å^3$)
C_{mn}	Concentrations of mobile helium species
C_{01}	Concentration of helium interstitial atoms
C_{10}	Concentration of vacancies
C_{11}	Concentration of helium substitutional atoms
C_{20}	Concentration of di-vacancie
C_I	Concentration of self-interstitial atoms
C_{He}^{e}	Thermal equilibrium concentration of helium interstitial atoms
C_V^e	Thermal equilibrium concentration of vacancies
C_I^e	Thermal equilibrium concentration of self-interstitial atoms
C_{He}^{e}	Pre-exponent constant of thermal formation of helium interstitial atoms
C_V^e	Pre-exponent constant of thermal formation of vacancies
C_I^e	Pre-exponent constant of thermal formation of self-interstitial atoms
ν_{He}^{o}	Pre-exponent constant of jump frequency of helium atoms (s^{-1})
ν_V^o	Pre-exponent constant of jump frequency of vacancies (s^{-1})
ν_I^o	Pre-exponent constant of jump frequency of self-interstitials (s^{-1})

ν_{He}	Jump frequency of helium atoms (s^{-1})
ν_V	Jump frequency of vacancies (s^{-1})
ν_I	Jump frequency of interstitials (s^{-1})
a_0	Lattice parameter (Å)
λ	Distance of nearest atoms (cm)
E^M	Activation energy for helium migration (eV)
E_V^T	Energy required to transfer a helium atom from substitutional site into a neighbouring vacancy (eV)
E_V^F	Formation energy of vacancies (eV)
E_{He}^F	Formation energy of helium interstitial atoms (eV)
E_I^F	Formation energy of self-interstitial atoms (eV)
E_V^M	Migration energy of vacancies (eV)
E_{He}^I	Migration energy of helium interstitial atoms (eV)
E_I^M	Migration energy of self-interstitial atoms (eV)
$E_{He,V}^B$	Binding energy of one helium atom and one vacancy (eV)
E_{He}^D	Detrapping energy of one helium atom from a substitutional position (eV)
G	Radiation damage rate (dpa s^{-1})
G_{He}	Helium production rate (appm s^{-1})
R_α^α	Reaction rate constant between defects α α can be helium interstitial atoms, vacancies, self-interstitial atoms or vacancy-helium complexes
E_{mn}^β	Thermal emission rate constant of defects β from mn-th vacancy-helium complexes β can be helium interstitial atoms or vacancies
K_α^α	Coordination number in R_α^α
K_{mn}^β	Coordination number in E_{mn}^β

P_α^k	Probability of trapping of point defect α jumping into sink of type k α can helium interstitial atoms, vacancies or self-interstitial atoms k can be dislocations, cavities or grain boundaries
ρ_d	Dislocation density (cm^{-2})
R_v	Average void radius (cm)
N_v	Number density of voids (cm^{-3})
R_g	Average grain radius (cm)
D_{He}^{tot}	Total diffusion coefficient of helium atoms taking into account dislocations and grain boundaries
D_{He}^{dl}	Diffusion coefficient of helium atoms in dislocations
D_{He}^{gb}	Diffusion coefficient of helium atoms in grain boundaries
E_{He}^{dl}	Activation energy of helium atoms migrating in dislocations
E_{He}^{gb}	Activation energy of helium atoms migrating in grain boundaries
δ	Average width of grain boundaries (cm)
x_d	Fractional concentration of atoms in dislocation core region
r_0	Radius of atoms (Å)
r_F	Recombination radius (Å)

Chapter 1

Introduction

1.1 Helium in fusion reaction

Fusion power offers the potential for almost limitless energy for future generations but it also presents some formidable scientific and engineering challenges. The energy is generated by a reaction:

$$^{2}_{1}\mathrm{D} + ^{3}_{1}\mathrm{T} \longrightarrow ^{4}_{2}\mathrm{He} + ^{1}_{0}\mathrm{n}(14\ \mathrm{MeV}) + \mathrm{Energy}$$

where D and T are deuterium and tritium respectively. Helium produced in the reaction is known to be practically insoluble in metals and alloys at thermal equilibrium. [1]. However, the high-energy neutron will knock the atoms in the surrounding materials and induce (n,α)-reactions [2, 3] such as

$$^{\mathrm{A}}_{\mathrm{Z}}\mathrm{M} + ^{1}_{0}\mathrm{n} \longrightarrow ^{\mathrm{A-3}}_{\mathrm{Z-2}}\mathrm{M} + ^{4}_{2}\mathrm{He}(\mathrm{several\ MeV})$$

Consequently, the first-wall materials in the fusion reactor are expected to contain a high concentration of helium atoms during and after irradiation. These helium atoms have a strong tendency to precipitate into helium-vacancy clusters and bubbles which are detrimental to the properties of metals and alloys. Studies [4, 5, 6] have shown that helium atoms assist the nucleation and growth of cavities in irradiated materials leading to volumetric swelling. Helium migration and clustering

at grain boundaries results in high temperature embrittlement [7, 8]. Tensile and other mechanical properties are all shown to be influenced by the presence of helium atoms [9, 10, 11]. Therefore, in designing materials for use in fusion reactors such as ITER (International Thermonuclear Experimental Reactor), it is necessary to investigate the property changes induced by the presence of helium atoms.

Amongst these problems, migration of helium atoms during irradiation is critical. Without understanding the migration mechanisms and consequent diffusion rates, it is not possible to account for the fate of helium atoms produced in the structural alloys. However, the migration mechanisms of helium atoms in metals undergoing radiation damage are rather complex. Some work [12, 13, 14, 15, 18, 21] has been done on inferring mechanisms from computer modelling of minimum energy lattice configurations and experiments with nickel, but a detailed study of helium migration in complex alloys such as steels would be welcomed. It is the objective of this study to establish a theoretical model which combines various mechanisms by which helium atoms migrate to yield an effective diffusion coefficient. Of particular interest is the diffusion of helium atoms in BCC (Body Centred Cubic)iron which is currently the best contender for first wall materials. It is an observed phenomenon that BCC metals show an overall slower swelling rate than FCC (Face Centred Cubic) metals under irradiation [22]. It is hoped that this work will explain why the swelling in BCC iron is delayed by investigating the the effective diffusion coefficient of helium atoms.

1.2 Diffusion of Helium Atoms

The presence of excess helium atoms is a basic requirement for bubble nucleation and growth. Their diffusion is the result of random jumps from one stable or metastable lattice site to another. The most important positions for He atoms in a lattice are interstitial sites and substitutional sites (He atoms in iron-vacancies). The preferred positions and dominant migration modes depend on temperature as well as on the presence of other intrinsic or irradiation induced defects acting as traps,

especially vacancies and He-vacancy clusters.The most important basic processes in He diffusion are interstitial migration, substitutional migration (vacancy migration) and the removal of a He atom from a vacancy or a He-vacancy cluster by thermal activation or some athermal mechanisms such as radiation induced re-solution, *i.e.* the helium atom is knocked out of the vacancy or the cluster during a neutron-induced cascade. The migration of He atoms can be characterized by a diffusion coefficient D^M_{He}

$$D^M_{He} = D^o \exp\{-E^M/kT\} \tag{1.1}$$

where D^o is a temperature-independent constant and is always given by

$$D^O = \frac{\nu^o_{He}\lambda^2}{6} \tag{1.2}$$

where ν^o_{He} is the vibrational frequency constant of helium atoms and λ is the distance of each jump which is equal to interatomic distance.
In eqn. (1.1), E^M is the activation energy of migration which can be determined by the slope of the Arrhenius plot of diffusion coefficient [23]; k is Boltzmann constant and T is temperature. In order to investigate different migration mechanisms, it is therefore necessary to determine the activation energy of helium jumping from one site to another. Based on experiments and computer simulations previous researchers [2, 17, 18, 19] have suggested that under different conditions, various mechanisms exist with a variety of migration energies E^M. This section will review the models of these migration mechanisms.

1.2.1 Interstitial diffusion mechanism

The simplest mechanism by which helium atoms transport is the interstitial diffusion mechanism, in which the atoms occupy and move between the interstitial sites, as shown in Fig. 1.1. The diffusion coefficient can be calculated using:

$$D^M_{He} = D^o \exp\{-E^I_{He}/kT\} \tag{1.3}$$

where E^I_{He} is the activation energy required for helium atoms to migrate interstitially. Philipps *et al.* [12, 13] suggested that even at very low temperatures *e.g.*

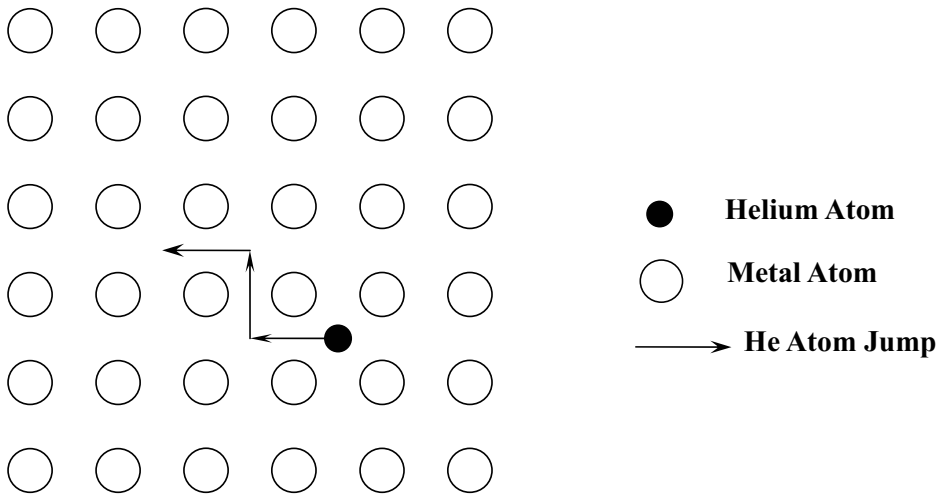

Figure 1.1: Interstitial diffusion mechanism of He atoms

77K, interstitial helium is mobile in nickel, indicating E^I_{He} as small as a few tenths of an eV. Results from computer simulations [20] compare well with the model.

1.2.2 Substitutional diffusion mechanism

Substitutional helium atoms occupy iron vacancies. Reed [15] concluded from simulations that helium atoms prefer to stay in the substitutional positions than in the interstitial positions because the energy required to place a helium atom into an interstitial position of the perfect BCC iron crystal 5.36 eV is considerably larger than that required to place it into an iron vacancy 1.61 eV. The difference between the two values 3.75 eV is defined as the binding energy of a helium atom with a vacancy $E^B_{He,V}$ [2]. The detrapping energy E^D_{He} is defined by the summation of $E^B_{He,V}$ and the activation energy of interstitial migration E^I_{He} explained in section 1.2.1, *i.e.*

$$E^D_{He} = E^B_{He,V} + E^I_{He} \tag{1.4}$$

which describes the energy required by a helium atoms to jump out of the vacancy and then migrate interstitially.

As can be seen, substitutional helium atoms all stay in the iron vacancies. However,

based on the different paths by which helium atoms transport, the substitutional migration mechanism can be subdivided into two categories:

(a) Vacancy mechanism

Migration of substitutional helium atoms by the vacancy mechanism is shown in Fig 1.2. A transient helium-vacancy complex containing one helium atom and two vacancies is formed in which He atom jumps from one vacancy to the other. The migration energy is hence calculated as [2]:

$$E^M = E_V^F + E_V^M + E_V^T \tag{1.5}$$

where E_V^F is the formation energy of a vacancy, E_V^M is the activation energy for a vacancy to migrate and E_V^T is the activation energy required to transfer a helium atom from a substitutional site into a neighbouring vacancy. Compared with the former two, the latter has a negligible value [2]. Under irradiation, this di-vacancy mechanism will be enhanced and the migration energy of helium is close to that of vacancy, e.g. $E^M \approx E_V^M$. Foreman and Singh [18] drew a similar conclusion in their work, finding that the diffusion coefficient of helium atoms is proportional to the concentration and the diffusion coefficient of vacancies:

$$D_{He}^M = ZC_V D_V \tag{1.6}$$

where Z is a coordination factor which reflects, but is not equal to, the number of sites from which the vacancy will spontaneously combine with the helium atom in the substitutional site. The calculation showed that for temperatures below half of the absolute melting temperature, helium diffusivity is enhanced by irradiation-produced vacancies.

(b) Dissociation mechanism

In this mechanism, a He atom in a metal-vacancy is dissociated from its position and diffuses interstitially until re-trapped by another metal-vacancy. The

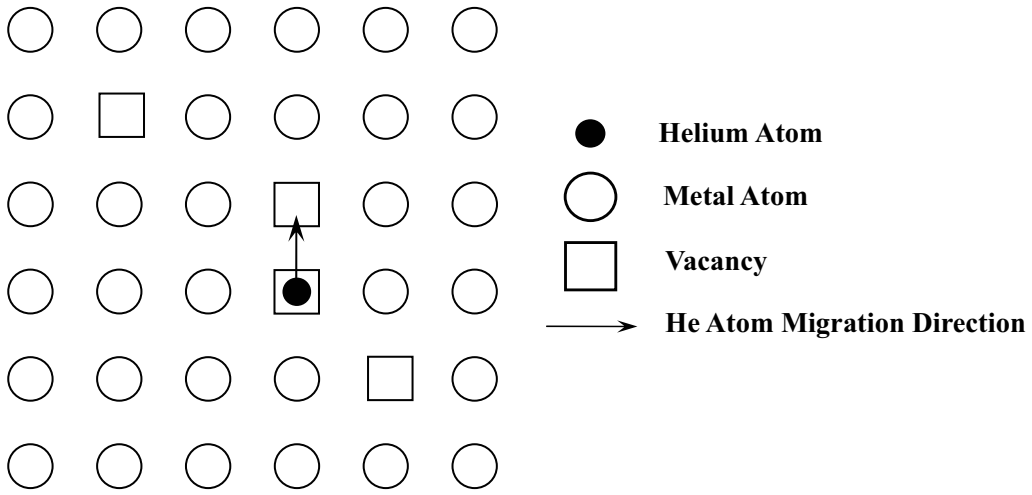

Figure 1.2: Substitutional diffusion mechanism of helium atoms

dissociation process can be activated thermally, by recombination of vacancies occupied by helium atoms with self-interstitial atoms or by irradiation-induced displacement, as shown in Figs. 1.3(a)–1.3(c).

In the absence of irradiation or at very high temperatures where thermal activation dominates, the measured activation energy for migration E^M is given by [2]:

$$E^M = E^B_{He,V} + E^I_{He} - E^F_V \tag{1.7}$$

where $E^B_{He,V}$ is the binding energy of a helium atom and a metal-vacancy. This mechanism will be preferred when helium-vacancy binding is not too strong and the vacancy formation energy is high, as is the case in nickel.
Trinkaus [17] suggested in a theoretical model that at high temperatures where the thermal vacancies outnumber the irradiation induced vacancies and the thermal dissociation process dominates, the diffusion coefficient of helium atoms can be given by:

$$D^M_{He} = D^I_{He}\exp\{-(G^B_{He,V} - G^F_V)/kT\} \tag{1.8}$$

where $G^B_{He,V}$ and G^F_V are the free energies for He-vacancy binding and vacancy formation respectively. D^I_{He} is the diffusion coefficient of helium migrating

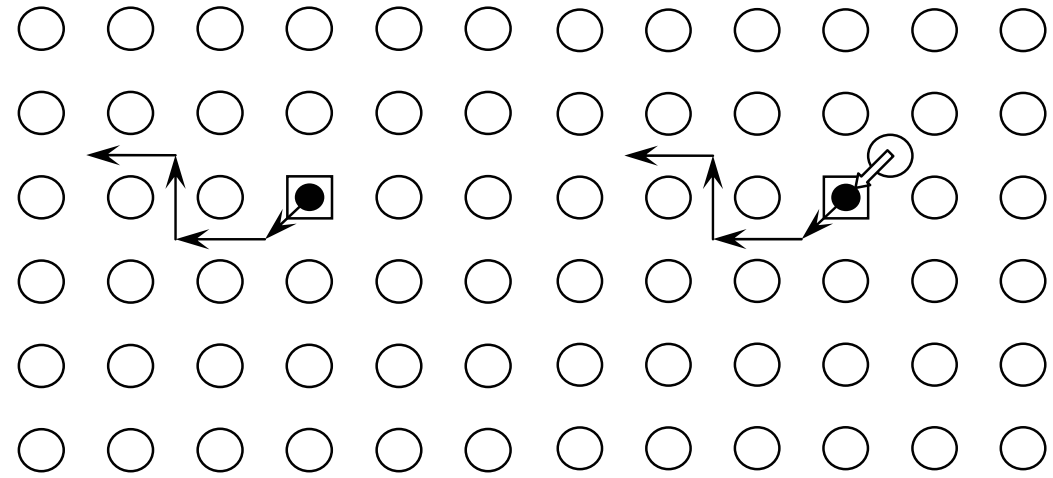

(a)

(b)

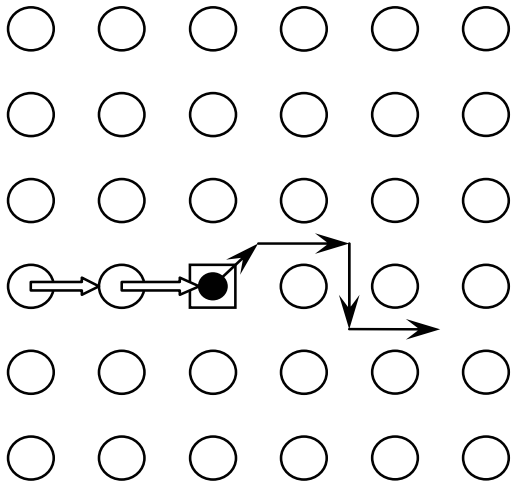

(c)

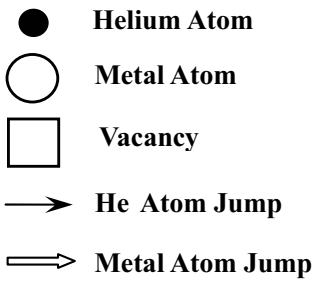

interstitial and is equivalent to D^M_{He} in eqn. (1.3). Since the free energy G^I_{He} is included in D^I_{He}, Eqn. (1.8) is essentially consistent with eqn. (1.7) [1]

At medium temperatures, where irradiation induced vacancies outnumber thermal vacancies but the dissociated mechanism is still governed by thermal activation (850 K $< T <$ 1030 K), D^M_{He} is given by

$$D^M_{He} \approx (\frac{4\pi r_F D_V}{\Omega G_{He}})^{1/2} D^I_{He} \exp\{-G^B_{He,V}/kT\} \tag{1.9}$$

where r_F is the recombination radius, Ω is the atomic volume, G_{He} is the helium production rate and D_V is the diffusion coefficient of vacancies.

At low temperatures, where irradiation induced vacancies are dominant and He dissociation from vacancies is governed by recombination (500 K $< T <$ 850 K), D^M_{He} is given by

$$D^M_{He} \approx D_V \tag{1.10}$$

It should be noted that eqn. 1.10 is valid based on experimental data from stainless steels. Over the same temperature range in aluminum alloys, Foreman *et al.* [18, 21] found the enhanced substitutional diffusion model described by eqn. (1.6) shows a better agreement with experiment observation. Radiation induced re-solution (Fig. 1.3(c)) has frequently been neglected in previous models. This is because under the irradiation conditions considered, the rate of release of trapped helium atoms via radiation-induced displacement events would lead to a very slow rate of helium diffusion by this mechanism. However, in fusion reactors, the high energy neutrons will induce significantly more displacement events so their effect may no longer be negligible. A re-solution parameter g was introduced to describe the dissociation by displacement events in Ghoniem and Takata's work [24]; it is the

[1] By thermodynamic definition, free energy G is a function of both enthalpy (activation energy) and entropy *i.e.* $G = E - TS$. Hence $\exp\{-G/kT\}$ can be derived as $A\exp\{-E/kT\}$ where A is a time-independent constant and equal to $\exp\{S/k\}$. So the energy term in eqn. (1.7) and (1.8) is consistent.

probability per second that a trapped helium atom will be struck out by a collision. The importance of the radiation mechanism is widely accepted for the swelling of nuclear reactor materials [25].

A simplified theory used by Reed [15] assumes that most traps are single vacancies and that helium atoms migrate interstitially between available traps. Therefore, if the helium atom moves from vacancy to vacancy, its average jump distance is best represented by the average distance between available vacancies i.e. $\lambda C_V^{-1/3}$ (λ is the distance between nearest atoms). The time spent by a helium atom in a vacancy ${\nu_0^{He}}^{-1}\exp\{E_{He}^D/kT\}$ is large compared with the time the atom spends in an interstitial position before encountering a vacancy, ${\nu_0^{He}}^{-1}C_V^{-1}\exp\{E_{He}^I/kT\}$ provided that C_V is sufficiently large. As explained previously, E_{He}^D is the detrapping energy and E_{He}^I is the activation energy for helium atoms to migrate interstitially. The helium diffusion constant can then be approximated by

$$D_{He}^M = \frac{\nu_0^{He}\lambda^2}{6} C_V^{-2/3}\exp\{-E_{He}^D/kT\} \tag{1.11}$$

It should be appreciated that the various diffusion mechanisms outlined above are mainly concerned with simple interactions between He atoms and vacancies under different conditions. They do not take into account extended defects such as dislocations, grain boundaries and precipitates, which exist in reality and make the investigation more complicated. In materials with complex microstructures such as steels, the effective diffusion coefficients may be either enhanced by particular migration paths, along dislocations or grain boundaries for instance, or reduced by trapping at impurity atoms, solid precipitates and voids or bubbles.

1.3 Summary

In this chapter, fusion reaction and material issues as well as the detrimental effects of helium on structural materials have been briefly introduced. Particular focus has been put on previous theories and models of mechanisms by which helium

atoms migrate. The migration mechanisms in complex alloys such as steels undergoing radiation damage are not well established, despite a strong technological need. The problem lies in the complicated paths by which helium can be transported. Suggested mechanisms include combinations of substitutional diffusion, interstitial diffusion, mutual (substitutional + interstitial) diffusion, momentum transfer and diffusion by vacancy-helium clusters. Additional possible reactions include:

1. Trapping/detrapping in single vacancies and higher-order vacancy complexes.
2. Trapping at dislocations and grain boundaries.
3. Replacement of substitutional helium with self-interstitials.
4. Clustering with other vacancies and helium.
5. Re-solution from traps by irradiation.

When dislocations, grain boundaries and cavities are taken into consideration, the problem becomes even more complicated. The purpose of this work was to contribute to a quantitative understanding of the helium migration mechanisms, especially in BCC iron which is known as the best contender for the first wall materials in fusion reactors. Therefore, interest is focused on trends in variation of the helium diffusion coefficient with crystal structures (BCC and FCC), temperatures, irradiation conditions and microstructure.

Chapter 2

Methodology

2.1 Effective Diffusion Model

Due to the various mechanisms by which helium atoms can transport inside the lattice, it is necessary to define an effective diffusion coefficient D_{He}^{eff} in the model, which is equal to the weighted average of individual diffusion coefficients. Mathematically, this can be expressed as [19]

$$D_{He}^{\text{eff}} \sum_{m=0}^{M} \sum_{n=0}^{N} C_{mn} = \sum_{m=0}^{M} \sum_{n=0}^{N} D_{mn} C_{mn} \tag{2.1}$$

where C_{mn} are the concentrations of mobile helium species with m and n representing the number of vacancies and the number of helium atoms respectively. For example, C_{01} is the concentration of helium transporting as interstitial atoms, C_{11} is the concentration of helium transporting as substitutional atoms (i.e. helium atoms trapped in a vacancy and migrating from one vacancy to another). D_{mn} are the corresponding diffusion coefficients. When $m, n > 1$, the terminology refers to vacancy-helium clusters.

The justification for eqn. (2.5) is as follows. If several mobile species migrate simultaneously via different mechanisms (Fig. 2.1), the total flux J is equal to a

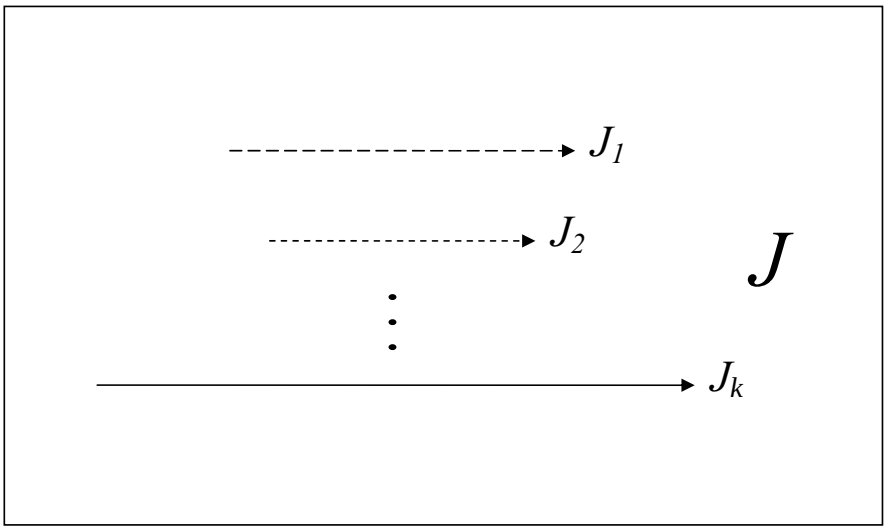

Figure 2.1: The effective diffusion model

weighted average of each flux J_i, *i.e.*

$$J = J_1 f_1 + J_2 f_2 + ... + J_k f_k = \sum_{i=1}^{k} J_i f_i \tag{2.2}$$

where f_i is the mole fraction of the ith mobile species. With Fick's first law:

$$J = -D\frac{dC}{dx} \tag{2.3}$$

where $\frac{dC}{dx}$ is the concentration gradient, one can easily obtain

$$D = \sum_{i=1}^{k} D_i f_i \tag{2.4}$$

For the mn-th mobile helium species, its mole fraction is equal to $C_{mn}/(\sum_{m=0}^{M}\sum_{n=0}^{N} C_{mn})$. Therefore, the effective helium diffusion coefficient in eqn. (2.1) can be obtained, to represent the diffusion coefficient of helium atoms measured in experiments.

Throughout this work, interstitial and substitutional helium atoms are, for simplicity, considered to be the only mobile helium species, so that

$$D_{He}^{\text{eff}} = \frac{D_{01}C_{01} + D_{11}C_{11}}{C_{01} + C_{11}} \tag{2.5}$$

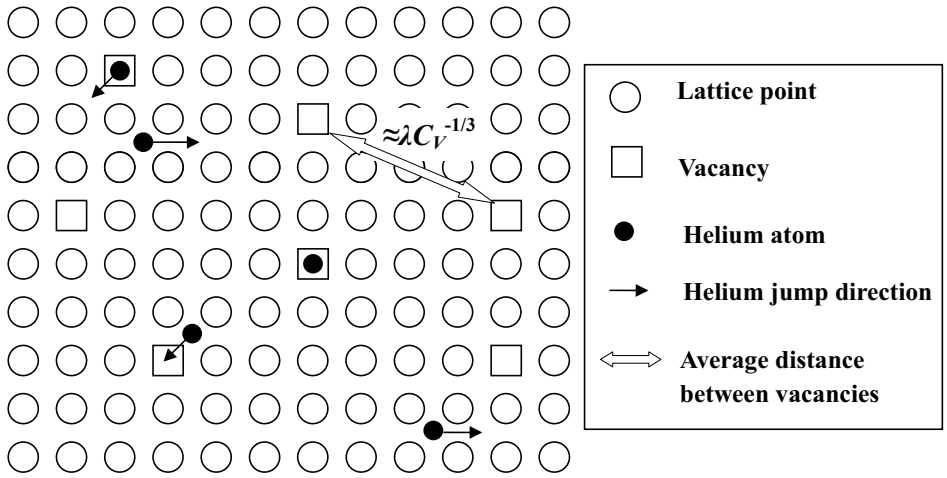

Figure 2.2: Simplified model of substitutional diffusion mechanism of helium atoms

where D_{01} is the diffusion coefficient of helium atoms transporting interstitially and can be given by:

$$D_{01} = \frac{\nu^o_{He}\lambda^2}{6}\exp\{-E^I_{He}/kT\} \tag{2.6}$$

where ν^o_{He} is the temperature-independent jump frequency of helium atoms, λ is the interatomic distance and E^I_{He} is the activation energy of interstitial migration. D_{11} is the diffusion coefficient of helium atoms transporting substitutionally. This can be calculated using [15]:

$$D_{11} = \frac{\nu^o_{He}\lambda^2}{6}C_V^{-2/3}\exp\{-E^D_{He}/kT\} \tag{2.7}$$

where E^D_{He} is the detrapping energy required when a helium atom in a metal-vacancy jumps out and migrate interstitially until being trapped again. When a helium atom migrates substitutionally with single vacancies as the abundant traps, the time it spends in a vacancy ${\nu^o_{He}}^{-1}\exp\{E^D_{He}/kT\}$ is large compared with that in an interstitial position before encountering a vacancy, ${\nu^o_{He}}^{-1}C_V^{-1}\exp\{E^I_{He}/kT\}$. The average jump distance can be therefore approximated as the average distance between vacancies, $\lambda C_V^{-1/3}$. The model is illustrated schematically in Fig. 2.2.

With respect to rapidly-moving helium atoms, vacancies in this process act as

stationary traps which will decrease the helium diffusion coefficient. This should be distinguished from the conventional vacancy diffusion mechanism occurring in metals in which vacancies are mobile species and hence the diffusion coefficient of metals usually increases as the density of vacancies increases.

2.2 Rate theory equations

To obtain a solution for eqn. (2.5), values for concentrations of interstitial and substitutional helium atoms as well as that of vacancies need to be known. They may vary with time under irradiation unless steady state exists. Besides, their values are strongly dependent on the reactions mentioned in the section 1.3. Chemical reaction rate theory has been used widely to determine the time-dependent concentrations of randomly migrating species [19, 24, 26, 6]. This approach includes all the possible reactions and involves the solutions of a set of differential equations. The following set of equations describe the time-dependent concentrations of a variety of helium-point defect clusters [19].
Unoccupied vacancies [1]:

$$\begin{aligned} dC_{10}/dt &= (1-\varepsilon)G + Z_V^d D_V \rho_d (C_V^e - C_{10}) + gGC_{11} + (R_{I,20}C_{20} - R_{I,10}C_{10})C_I + \\ &\quad \sum_{i=0}^{M}\sum_{j=0}^{N} (E_{ij}^V - R_{10,ij}C_{10})C_{ij} \end{aligned} \tag{2.8}$$

where dC_{10}/dt is the rate of change in concentration of unoccupied vacancies. $(1-\varepsilon)G$ is the rate at which mono-vacancies are induced by irradiation, since εG is the rate at which di-vacancies are induced and G is the radiation damage rate *i.e.* the rate at which vacancy-interstitial pairs Frenkel pairs are induced. $Z_V^d D_V \rho_d (C_V^e - C_{10})$ is the rate at which excess vacancies $(C_V^e - C_{10})$ sink at dislocations. gGC_{11} is the rate at which helium atoms are knocked out of the substitutional sites by the radiation displacement and become interstitials. $R_{I,20}C_{20}C_I$

[1] In this thesis, vacancies only mean mono-vacancies, not including di-vacancies unless specified

and $R_{I,10}C_{10}C_I$ are the rates at which SIAs react with di-vacancies and with mono-vacancies respectively. The former will generate unoccupied vacancies and the latter annihilate them.$\sum_{i=0}^{M}\sum_{j=0}^{N} E_{ij}^{V}C_{ij}$ is the rate at which vacancies are thermally emitted from ij-th vacancy-helium clusters;$\sum_{i=0}^{M}\sum_{j=0}^{N}(R_{10,ij}C_{10}C_{ij}$, on the contrary, is the rate at which vacancies react with ij-th clusters and generate $i+1, j$-th clusters. A detailed explanation of the meaning and the derivation of each symbol will be given after eqn. (2.12).

SIAs (Self-interstitial atoms):

$$dC_I/dt = G - \sum_{i=0}^{M}\sum_{j=0}^{N} R_{I,ij}C_{ij}C_I - Z_I^d\rho_d C_I - 2R_{I,I}C_I^2 \tag{2.9}$$

where G is the rate at which SIAs are induced by irradiation;$\sum_{i=0}^{M}\sum_{j=0}^{N} R_{I,ij}C_{ij}C_I$, $Z_I^d\rho_d C_I, 2R_{I,I}C_I^2$ are the rates at which SIAs are annihilated respectively by reactions between SIAs and ij-th clusters, by reactions between two SIAs, and by dislocations as sinks.

Interstitial heliums:

$$\begin{aligned} dC_{01}/dt = {} & G_{He} - Z_{He}^d\rho_d D_{He}(C_{01} - C_{He}^e) - R_{10,01}C_{10}C_{01} + R_{I,11}C_I C_{11} + \\ & \sum_{i=0}^{M}\sum_{j=0}^{N}(E_{ij}^{He} + jgG - R_{01,ij}C_{01})C_{ij} \end{aligned} \tag{2.10}$$

where all the terms are similar to those of vacancies except G_{He} is the helium production rate rather than the radiation damage rate G.

Di-vacancies:

$$\begin{aligned} dC_{20}/dt = {} & 0.5(\varepsilon G + R_{10,10}C_{10}^2) - \sum_{i=0}^{M}\sum_{j=0}^{N} R_{ij,20}C_{ij}C_{20} - Z_{20}^d D_{20}\rho_d C_{20} - \\ & R_{I,20}C_I C_{20} - E_{20}^V C_{20} + E_{30}^V C_{30} + R_{I,30}C_I C_{30} + E_{21}^{He}C_{21} \end{aligned} \tag{2.11}$$

Clusters containing m-vacancies and n-helium atoms:

$$\begin{aligned} dC_{mn}/dt &= E^{He}_{m,n+1}C_{m,n+1} + (E^{V}_{m+1,n} + R_{I,m+1,n}C_I)C_{m+1,n} + \sum_{\substack{i+k=m \\ j+l=n}} R_{ij,kl}C_{ij}C_{kl} - \\ & (Z^{d}_{mn}D_{mn}\rho_d + ngG + R_{I,mn}C_I + E^{He}_{mn} + E^{V}_{mn})C_{mn} - \\ & \sum_{i=0}^{m}\sum_{j=0}^{n} R_{ij,mn}C_{ij}C_{mn} \end{aligned} \tag{2.12}$$

which gives all the reactions involving clusters in a general form. $E^{He}_{m,n+1}C_{m,n+1}$ is the rate at which $m, n+1$-th clusters emit a helium atom and then become mn-th clusters; $(E^{V}_{m+1,n} + R_{I,m+1,n}C_I)C_{m+1,n}$ are the rates at which $m+1, n$-th clusters lose a vacancy by thermal emission and by replacement of a SIA respectively and then become mn-th clusters; $\sum_{\substack{i+k=m \\ j+l=n}} R_{ij,kl}C_{ij}C_{kl}$ is the rate at which small clusters coalescence to form mn-th clusters; $(Z^{d}_{mn}D_{mn}\rho_d + ngG + R_{I,mn}C_I + E^{He}_{mn} + E^{V}_{mn})C_{mn}$ are the rates at which mn-th clusters disappear by different mechanisms including by dislocations, by radiation displacement, by reactions between SIAs and mn-th clusters, and by thermal emission of a helium atom or a vacancy; $\sum_{i=0}^{m}\sum_{j=0}^{n} R_{ij,mn}C_{ij}C_{mn}$ is the rate at which mn-th clusters react with any other clusters.

Further explanation of each parameters in eqn. (2.8–2.12)is given as follows. C_α is the concentration of defect α which can represent any of species in eqn. (2.8–2.12). The superscript e denotes concentrations at thermal equilibrium. The thermal equilibrium concentration *e.g.* C^e_V can be calculated using:

$$C^e_V = C^o_V \exp\{-E^F_V/kT\} \tag{2.13}$$

where C^o_V is the formation pre-exponent factor and E^f_V is the formation energy.
In eqn. (2.8–2.12) D_α is the diffusion coefficient of each species; G is the radiation damage rate, i.e. the generation rate of Frenkel pairs; G_{He} is the helium production rate; ε is the fraction of vacancies produced directly as di-vacancies by irradiation; g is the re-solution parameter and is defined as the probability per second that a

trapped helium atom will be struck out by a collision [24]. This parameter essentially describes the possible effect of high-energy neutrons on the helium diffusion directly or indirectly.

Z_α^d is the line dislocation bias factor for defect α. This factor, when multiplied by the concentration of densities ρ_d, can be used as an approximation of the strength of line dislocations as sinks for each mobile species. In above equations, the line dislocations are considered as the only sinks. However, sinks of other types such as cavities, precipitates or grain boundaries can also be included. Investigation of their effects on the effective diffusion coefficient of helium atoms D_{He}^{eff} will be explained in section 3.4.

$R_{ij,mn}$ are the reaction rate constant between ij-th clusters and mn-th clusters. Likewise, $R_{I,mn}$ is the reaction rate constant between SIAs and mn-th clusters. By including these rate constants, reactions such as the recombination of vacancies with self-interstitials ($R_{I,10}$), the replacement of helium atoms trapped in vacancies by self-interstitials ($R_{I,11}$), the clustering of helium atoms and vacancies or their clusters ($R_{ij,mn}$) can be taken into consideration. The reaction rate constants can be calculated using [27]:

$$R_{\alpha,mn} = K_{mn}^{\alpha} \nu_{\alpha}^{o} \exp\{-E_{\alpha}^{M}/kT\} \tag{2.14}$$

where ν_α^o is the pre-exponent constant of jump frequency of defect α; E_α^M is the migration energy of defect α, which for interstitial helium atoms, for instance, is equal to E_{He}^I; K_{mn}^α is the combinatorial number which describes the number of sites from where defect α may jump into the mn-th clusters, leading to the reaction. Some references [28, 29, 30] have given methods for determining K_{mn}^α. Among them, Wiedersich [30] assumed K_{mn}^α to be 12 when considering a model with a FCC structure. Therefore, it is reasonable to approximate K_{mn}^α as the number of nearest atoms.

E_{mn}^β is the emission rate of the point defect β from the mn-th clusters. In reality only single vacancy or helium atom are be thermally emitted from clusters. E_{mn}^β is

given by [19]:

$$E^{\beta}_{mn} = K^{\beta}_{mn}\nu^{o}_{\beta}\exp\{-(E^{B}_{\beta,mn} + E^{M}_{\beta})/kT\} \tag{2.15}$$

where K^{β}_{mn} can be assumed to be equal to K^{α}_{mn}. $E^{B}_{\beta,mn}$ is the binding energy of the last defect β in the mn. $E^{B}_{He,V}$, for instance, is the binding energy of single helium atom and vacancy.

2.3 Simplified helium diffusion model

In this work, eqns. (2.8–2.12) have been used, together with eqn. (2.5), to determine the effective diffusion coefficient as a function of parameters such as temperatures, radiation damage, *etc.*. However, modifications have been made so that the model can be simplified without losing the essential physical meanings. These modifications include:

- The system is considered to contain interstitial helium atoms, substitutional helium atoms, vacancies, self-interstitials, dislocations and uniformly distributed cavities characterized by an average cavity radius and a number density. Grain boundaries is taken into account by using an average grain size.

- The model is designed for the steady state. Clustering, di-vacancy population and nucleation of helium bubbles or cavities are assumed negligible. The model should therefore be best used in the incubation period of cavities before their growth. It should be also used as a 'snapshot' of how the void radius might affect the diffusion of helium atoms.

Based on these assumptions, the modified steady-state rate equations are expressed as:
Unoccupied vacancies:

$$G + E^{He}_{11}C_{11} + gGC_{11} - R_{I,10}C_{10}C_I - R_{01,10}C_{01}C_{10} + \nu_V P_V(C^{e}_{V} - C_{10}) = 0 \tag{2.16}$$

SIAs:

$$G - R_{I,10}C_{10}C_I - R_{I,11}C_{11}C_I + \nu_I P_I(C_I^e - C_I) = 0 \tag{2.17}$$

Interstitial helium atoms:

$$G_{He} + E_{11}^{He}C_{11} + R_{I,11}C_IC_{11} - R_{01,10}C_{01}C_{10} + \nu_{He}P_{He}(C_{He}^e - C_{01}) = 0 \tag{2.18}$$

Substitutional helium atoms:

$$R_{01,10}C_{10}C_{01} - E_{11}^{He}C_{11} - R_{I,11}C_IC_{11} - gGC_{11} = 0 \tag{2.19}$$

In eqns. (2.16)–(2.19), the left-hand sides are equal to zero, given the steady state. Another factor that must be taken into account during the study of helium migration is the existence of extended defects in irradiated materials such as dislocations, grain boundaries and voids which act as point defect sinks. This is incorporated in the model by introducing the parameter P_α, the probability that a point defect α will be removed from the system at a sink. Each probability P_α^k depends on the type, geometry and density of sinks of type k, but not on the jump frequency of the point defects or their concentrations. For the evaluation of the steady state conditions in this model, the total probability P_α is given by:

$$P_\alpha = \sum_k P_\alpha^k \tag{2.20}$$

where k represents dislocations, voids, or grain boundaries. In this way, the effect of these sinks on the effective helium diffusion coefficient can be investigated. Wiedersich [30] gave mathematical expressions for the probability of each type sink:
Dislocations:

$$P^d = \frac{1.5\lambda^2\pi\rho_d}{\ln(\pi\rho_d^{-0.5}\lambda^{-1}) - 1} \propto \lambda^2\rho_d \tag{2.21}$$

Cavities or precipitates:

$$P^v = \frac{2\lambda^2\pi N_v}{3R_v^{-1} - 7.2\pi N_v} \tag{2.22}$$

Grain boundaries:

$$P^{gb} = \frac{2.5\lambda^2}{R_g^2} \tag{2.23}$$

In eqns. (2.21–2.23), ρ_d is the dislocation density; R_v and N_v are the average radius and the number density of cavities or precipitates respectively; R_g is the average size of grains. Braisford [32] has developed comprehensive, but more complicated theoretical models for sink strength, which show similar results. For simplicity, Wiedersich's model will therefore be used in this work.

All the parameters in eqns. (2.16)–(2.19) are known except the concentrations of the four species. They must be obtained by simultaneous solution. Although this is a relatively simple system, it is still not easily amenable to analytical solutions. A FORTRAN subroutine [31] employing an implicit numerical integration algorithm will be used to obtain numerical solutions. All the data required in the calculation are compiled in table 2.1.

2.4 Review

In this chapter, the concept of an effective diffusion coefficient of helium atoms was introduced. A theoretical method to obtain this value was developed using the rate theory equations. Parameters involved in the rate equations were comprehensively explained. A new theoretical model was developed by modifying the general time-dependent rate equations so that some necessary simplifications can be achieved. FORTRAN subroutine DLSODE was used to solve eqns. (2.16)–(2.19) and numerical results are discussed in next chapter.

Symbol	Definition	Value	Unit	Ref.
k	Boltzmann's constant	8.617×10^{-5}	eV/K	
a_0	Lattice parameter	2.87	Å	
E_V^F	Formation energy of vacancies	1.5	eV	[2]
E_{He}^F	Formation energy of helium interstitial atoms	5.36	eV	[15]
E_I^F	Formation energy of self-interstitial atoms	4.08	eV	[33]
E_{He}^M	Migration energy of helium interstitial atoms	0.17	eV	[15]
E_V^M	Migration energy of vacancies	0.55	eV	[2]
E_I^M	Migration energy of self-interstitial atoms	1.09	eV	[36]
$E_{He,V}^B$	Binding energy of helium and vacancy	3.75	eV	[2]
E_{He}^D	Detrapping energy of helium substitutional atoms	3.92	eV	[15]
ν_{He}^o	Frequency pre-exponent of helium atoms	5×10^{14}	(s^{-1})	[36]
ν_V^o	Frequency pre-exponent factor of vacancies	5×10^{13}	(s^{-1})	[30, 33]
ν_I^o	Frequency pre-exponent of self-interstitials	5×10^{12}	(s^{-1})	[34]
C_{10}^o	Formation pre-exponent of vacancies	4.48	at/at	[35]
C_{01}^o	Formation pre-exponent of helium interstitial atoms	5	at/at	[30]
C_I^o	Formation pre-exponent of self-interstitial atoms	5	at/at	[30]
K_{mn}^{α}	Combinatorial number	8		
g	Re-solution parameter	1×10^{-6}		[24]

Table 2.1: Data for BCC iron used to solve eqns. (2.16)–(2.19)

Chapter 3

Results and Discussion

3.1 Steady state concentrations

The concentrations of species inside the irradiated materials such as the the concentration of vacancies C_{10}, concentration of interstitial helium atoms C_{01} *etc.* are key in determining the effective helium diffusion coefficient of helium atoms. This section will discuss these concentrations obtained using the rate theory eqns. (2.16)–(2.19). This will provide a basis for further discussion of the different diffusion mechanisms.

Fig 3.1 shows the steady state concentrations of the four species in eqns. (2.16)–(2.19) varying with temperature at a constant radiation damage rate $G = 10^{-6}$ dpa s^{-1} and a constant helium production rate $G_{He} = 10^{-6}$ appm s^{-1}. The terminology is the same as in last chapter, *i.e.*, $C_{10}, C_I, C_{01}, C_{11}$ are the concentrations of unoccupied vacancies, SIAs (self-interstitial atoms), interstitial helium atoms and substitutional helium atoms respectively.

The vacancy concentration C_{10} slightly decreases in the lower temperature region with increasing temperature, goes through a minimum and then becomes indistinguishable from the thermal equilibrium concentration C_V^e in the high temperature region as the tangent gradient in the high temperature region is equal to the formation energy of vacancies E_V^F, *i.e.* 0.55eV in BCC iron. This is because in the

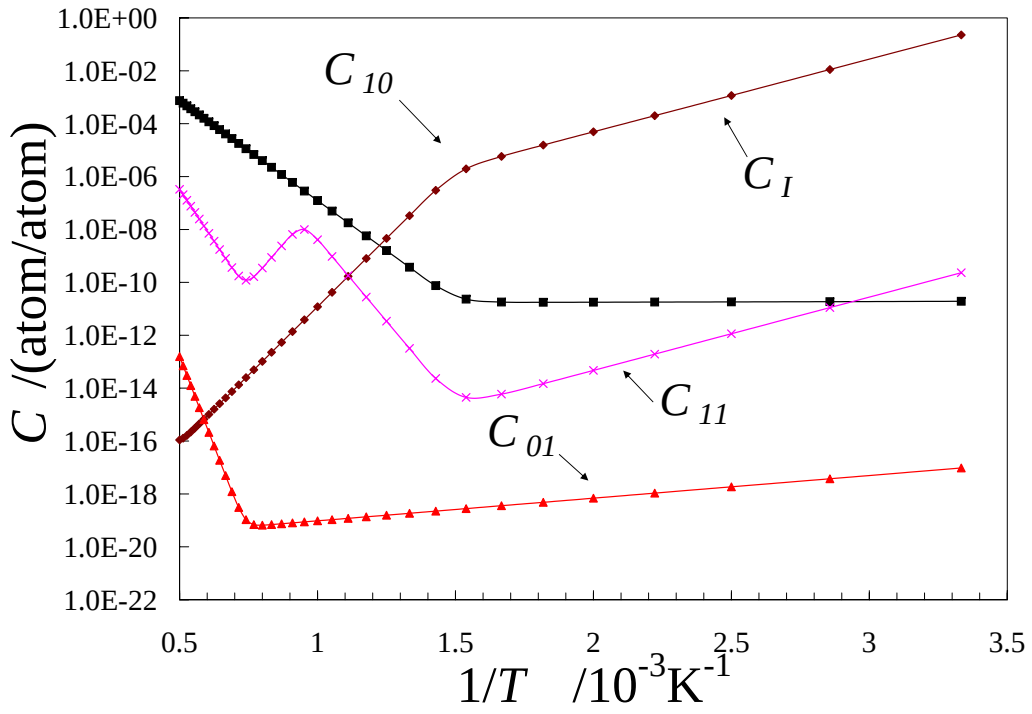

Figure 3.1: Steady state concentrations of mobile species as a function of temperature : C_{10} the concentration of unoccupied vacancies, C_I the concentration of SIAs, C_{01} the concentration of interstitial helium atoms, C_{11} the concentration of substitutional helium atoms

lower temperature region most vacancies are generated by radiation damage while in the high temperature region, thermal induced vacancies will outnumber vacancies induced by the radiation damage.

The concentration of SIAs (self-interstitial atoms) C_I has the similar general features. It decreases with increasing temperature. A minimum is supposed to appear at rather hight temperatures due to the relatively high formation energy, indicating the starting point of the dominance of thermal induced SIAs. However, within the temperature range investigated in this work (2000 K $> T >$ 300 K), the minimum is absent, which means the radiation damage dominates the generation of SIAs. The reduced slope in the low temperature *i.e.* below 700 K are the consequence of the fact that reactions between SIAs and other species such as vacancies and substitutional helium atoms become significant. The general features of C_{10} and C_I varying with temperature are consistent with Wiedersich's work [30]. However, in his work, data in the calculation were for a FCC structure material nickel and the interactions of SIAs and vacancies with helium atoms were ignored, which may explain the differences in detail between Fig. 3.1 and his work.

The features of the concentration of interstitial helium atoms C_{01} are similar to those of C_{10} since the mechanisms that interstitial helium atoms and vacancies are produced and annihilated are more or less the same. The formation energy of interstitial helium atoms at thermal equilibrium, 5.36 eV in BCC iron, is much higher than that of vacancies are much higher so that $C_{01} \ll C_{10}$ and the minimum point for C_{01} appears at a higher temperature. However, if dislocations and grain boundaries are taken into consideration, the fates of the two species are treated differently in this system. It is assumed that vacancies will be annihilated in these sinks while helium atoms can diffuse rapidly inside them and be thermally emitted. The effect of dislocations and grain boundaries on the effective diffusion coefficient will be investigated in section 3.4.

The features of the concentration of substitutional helium atoms C_{11} is complex.

By deriving eqn. 2.19, C_{11} can be given as:

$$C_{11} = \frac{R_{01,10}C_{10}C_{01}}{E_{11}^{He} + gG + R_{I,11}C_I} \tag{3.1}$$

The numerator describes the production process of substitutional helium atoms and the three terms in the denominator describe the three dissociation process which are the thermal emission E_{11}^{He}, the replacement of SIAs $R_{I,11}C_I$ and the direct displacement from irradiation cascades gG as explained in section 1.2.2. E_{11}^{He} outweighs the other two when temperatures are high, above 1000 K. In this high temperature region, the production rate $R_{01,10}C_{10}C_{01}$ exceeds the dominant thermal emission rates E_{11}^{He} at even high temperatures, *i.e* above 1350 K and becomes less below that, which explains the minimum at the high temperature region. When temperatures are relatively low, less than 1000 K, the term $R_{I,11}C_I$ will dominate the emission process, *i.e*, most helium atoms are emitted out of the substitutional positions by the replacement of SIAs rather than by the thermal activation. Again, the minimum point in the low temperature region arise from the competition between the production process and the annihilation process. The term describing the emission by the radiation displacement gG becomes significant only at very low temperatures *e.g.* below 300 K or very high damage rates *e.g.* 1 dpa s^{-1} and therefore is negligible in this model.

The two concentrations concerning helium atoms C_{01} and C_{11} in Fig. 3.1 show a large difference of several orders of magnitude. At steady state, most helium atoms stay in the substitutional positions which are energetically favorable [15]. As a consequence, when calculating the effective diffusion coefficient D_{He}^{eff} using eqn. (2.5), C_{01} in the denominator can always be neglected. Besides, the dissociation energy E_{He}^{D}, 3.92 eV, is significantly higher than the migration energy of interstitial helium atoms E_{He}^{M}, 0,17 eV, so the substitutional diffusion coefficient D_{11} is smaller than the interstitial diffusion coefficient D_{01} by several orders of magnitude. $C_{11}D_{11}$ is at most one tenth of $C_{10}D_{01}$ when T is below 300 K and therefore can be neglected from the numerator. Eqn. (2.5) can be simplified as:

$$D_{He}^{\text{eff}} = \frac{D_{01}C_{01}}{C_{11}} \tag{3.2}$$

That is, the effective diffusion coefficient of helium atoms D_{He}^{eff} is mainly dependent on the diffusion coefficient of interstitial helium atoms D_{01} and the ratio of the concentration of interstitial helium atoms C_{01} to the concentration of substitutional helium atoms C_{11}. In the following sections, discussion of effects of various factors on D_{He}^{eff} will be based on this conclusion.

3.2 Effect of different crystal lattices on D_{He}^{eff}

Austenitic stainless steels and Ni-based alloys have been successfully employed in the fission nuclear reactors. They both possess a FCC crystal structure. However, experiments [22] show that swelling in BCC structure materials is much delayed as compared with FCC counterparts. Besides, previous work [37] have found that the mechanical properties of FCC steels such as yield strength, UTS, and toughness deteriorate dramatically with an increased helium production, as is expected to occur in the fusion reactors. The application of BCC structure materials such as ferritic steels were therefore suggested. In this section, comparison of D_{He}^{eff} between BCC steels and FCC steels is made in order to help explain the different behaviours of these structures.

3.2.1 FCC model

The model has been initially used to calculate the effective diffusion coefficient of a FCC structure material *e.g.* nickel. It is hoped that in this way the validation of the model can be achieved by comparing the results with those from previously published work. Calculations based on BCC structure materials such as ferrite steels have never been attempted and are presented after the validation of the model. The main differences between BCC and FCC structures, for the purposes of this model, are the values of different energies. The interstitial jump distance λ and the coordination numbers K_{mn}^{α} also vary with the crystal structure. However, their effect on the diffusion coefficient is not comparable with that of energies which

may change the magnitude of the diffusion coefficient in orders. Table 3.1 lists the different data used in two models:

Fig. 3.2 shows the effective coefficient of helium atoms in a FCC structure material

	a_0 (Å)	E_V^F (eV)	E_V^M (eV)	E_{He}^M (eV)	$E_{He,V}^B$(eV)	E_{He}^D(eV)	K_{mn}^{α}
FCC	3.52	1.8 [38]	1.4 [38]	0.20 [2]	2.96 [24]	3.16 [24]	12
BCC	2.87	1.5	0.55	0.17	3.75	3.92	8

Table 3.1: Data used in the BCC model and the FCC model

varying with temperature under irradiation condition of constant radiation damage rate $G = 10^{-6}$ dpa s^{-1} and constant helium production rate $G_{He} = 10^{-6}$ appm s^{-1}. Fig. 3.2(a) shows the result obtained from this work and Fig. 3.2(b) is the result from other published work [19]. They show acceptable agreement in both the trend and the magnitude, especially in the intermediate temperature region 1000 K $> T >$ 600 K. However, the detailed differences at high temperatures 1000 K $< T$ and at low temperatures 400 K $> T$ should be appreciated. It is because in the published work, more species such as di-vacancies and complex vacancy-helium clusters are included which gives extra accuracy that is not necessary in this work.

3.2.2 Comparison of BCC model and FCC model

Fig. 3.3 shows the effective diffusion coefficients of helium atoms varying with temperature in both BCC and FCC structure materials. The effective diffusion coefficient varies dramatically with different crystal structures. Especially in BCC steels, at the temperature range of 600 K–1000 K, D_{He}^{eff} increases as the temperature decreases, indicating a negative effective migration energy. When the temperature is below 800 K, D_{He}^{eff} in BCC steels is higher than that in FCC counterpart by several orders of magnitude. To explain the apparent abnormality, Fig. 3.4 is given, which shows the concentration of interstitial helium atoms C_{01} and the concentration of substitutional helium atoms C_{11} varying with temperatures in both BCC

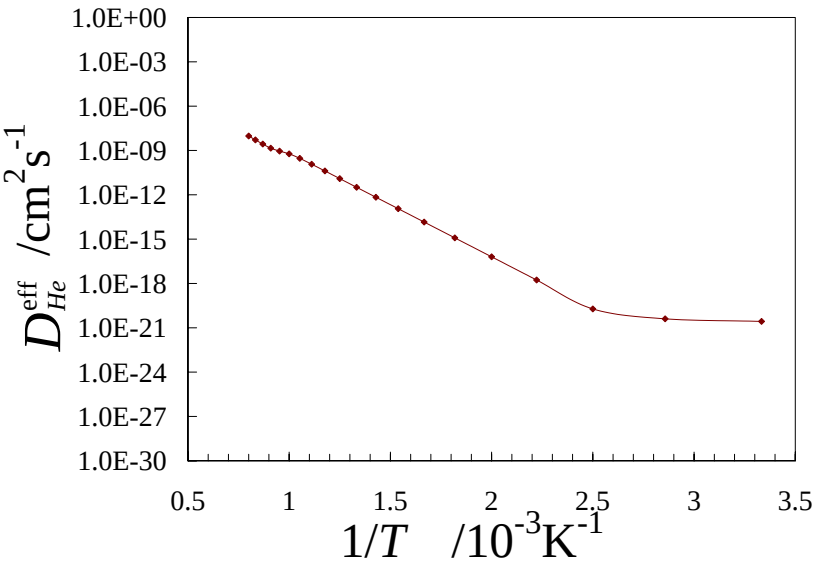

(a)

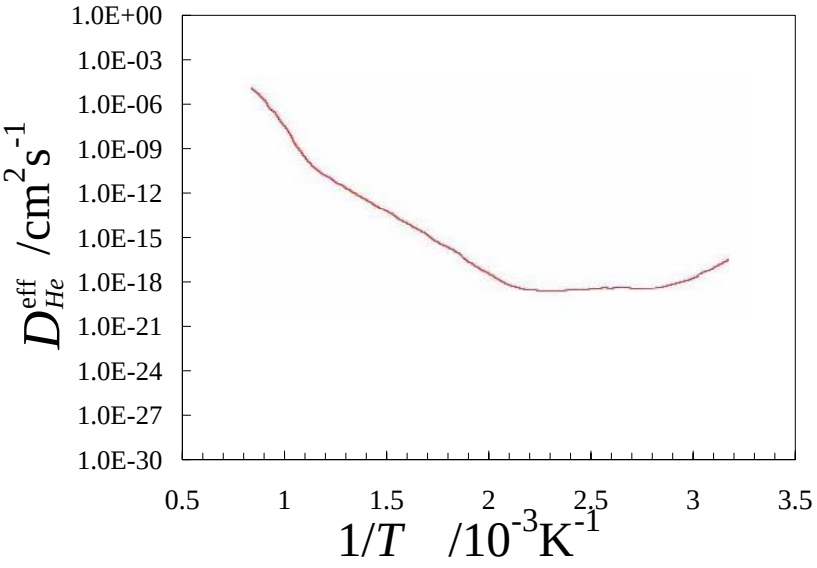

(b)

Figure 3.2: Effective coefficients of helium atoms as a function of temperature in a FCC structure material: (a) Results from this model. (b) Results from previously published paper [19]

.

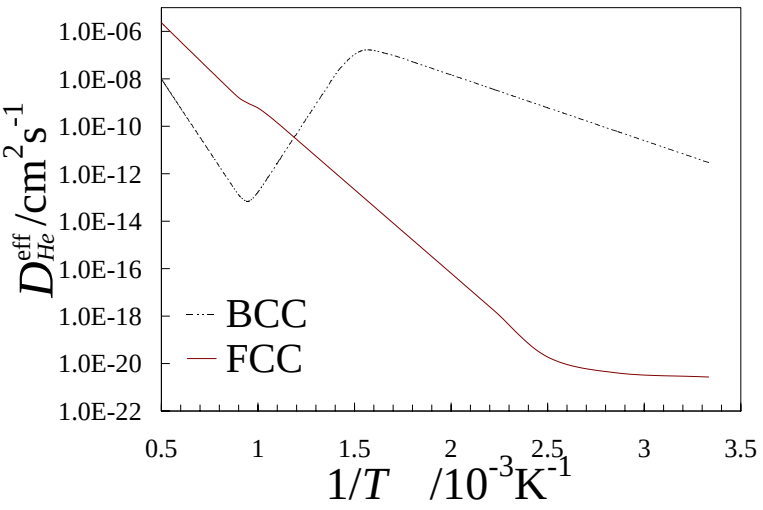

Figure 3.3: Comparison between FCC and BCC structure materials in effective diffusion coefficient of helium atoms as a function of temperature

and FCC structure materials.

As can be seen in the fig. 3.4, C_{01} does not changes with different crystal structures. The change in D_{He}^{eff} arises from the variation of C_{11}. As discussed in section 3.1, the production of substitutional helium atoms is determined by the reaction between interstitial helium atoms and unoccupied vacancies, *i.e.* $R_{10,01}C_{10}C_{01}$ and the annihilation of substitutional helium atoms (the emission of helium atoms from the substitution position) is dominated by the thermal emission E_{11}^{He} at temperature above 1200 K and by the replacement of SIAs $R_{I,11}C_I$ below that. According to eqns. (2.14)–(2.15), these terms are closely related to the detrapping energy E_{He}^{D} and the migration energy of vacancies E_V^M which are significantly different in BCC and FCC structure materials as listed in table 3.1

In the high temperature region ($T > 1200$ K), C_{11} in BCC is significantly higher than that in FCC due to a relatively large E_{He}^{D}. As more helium atoms are trapped in vacancies, D_{He}^{eff} in BCC is consequently lower than in FCC.

In the low temperature region ($T < 600$ K), a relatively smaller magnitude of E_V^M

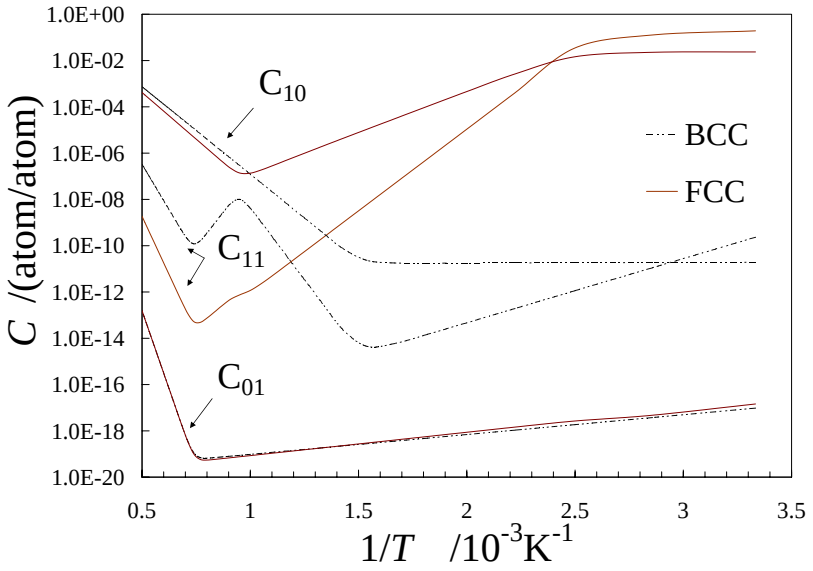

Figure 3.4: Concentration of interstitial helium atoms and the concentration of substitutional helium atoms as a function of temperature in BCC and FCC structure materials

in BCC (0.55 eV as opposed to 1.2 eV in FCC) results in a lower concentration of vacancies at steady state as vacancies are annihilated at sinks more rapidly. Correspondingly C_{11} at steady state lowers in BCC, leading to a relatively higher D_{He}^{eff}. In the intermediate temperature region (1200 K $>$ T $>$ 600 K), the apparent negative effective diffusion coefficient results from the decreasing of C_{11} with the decreasing temperatures. The dependence of C_{11} on both E_{He}^{D} and E_{V}^{M} are complicated. However, it is reasonable to conclude that the relatively large E_{He}^{D} and small E_{V}^{M} of BCC steels leads to the negative effective activation energy for diffusion in this temperature region.

3.3 Effect of irradiation conditions on D_{He}^{eff}

Structural materials used in nuclear reactors will be subjected to severe irradiation damage, especially in the fusion reactors. The parameters normally employed

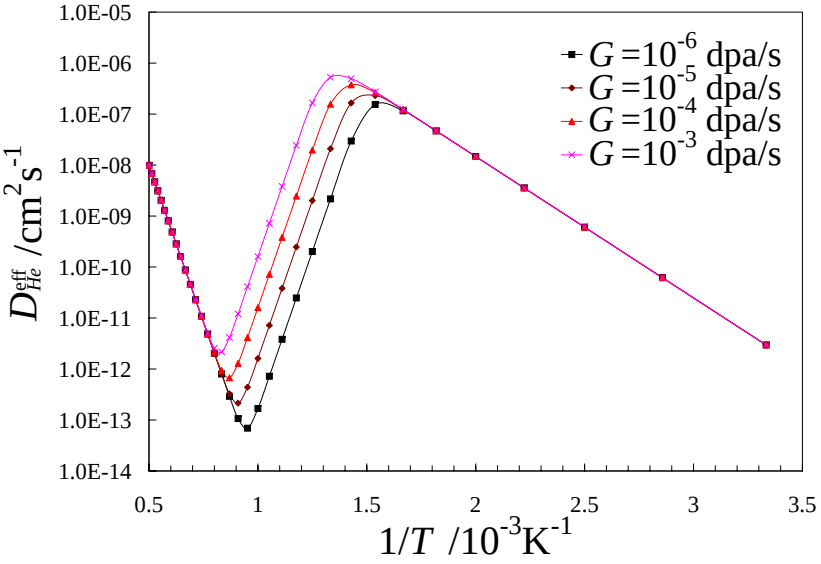

Figure 3.5: Effective diffusion coefficient of helium atoms as a function of temperature

to characterize the irradiation conditions are temperature T, radiation damage rate G and helium production rate G_{He}. In this section, the influence of these parameters on the effective diffusion coefficient D_{He}^{eff} are investigated, using the model of BCC steels.

3.3.1 Effect of radiation damage rate

Fig. 3.5 shows the effective diffusion coefficient of helium atoms D_{He}^{eff} varying with temperature at different radiation damage rates G. It seems that the G has a significant effect only at the temperature range 600 K–1200 K which is supposed to be service temperatures in fusion reactors. This is verified by Fig. 3.6 which shows the effective diffusion coefficient as a function of G at different temperatures.

Clearly, D_{He}^{eff} increases with an increasing G. Especially in the temperature range 800 K $\sim$ 600 K, the effect of G is exponential in the order of unity (note that y-axis in Fig. 3.6(c) and Fig. 3.6(d) is on a logarithmic scale, opposite to the rest).

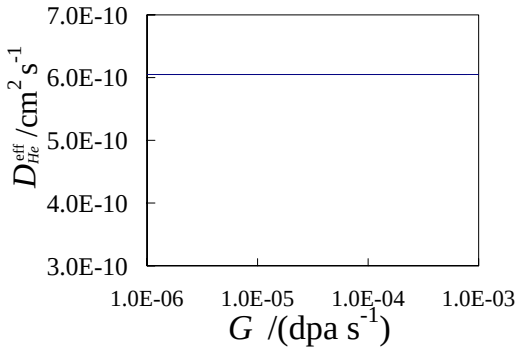

(a) T=400 K

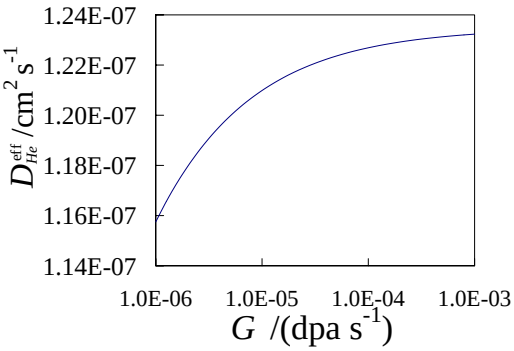

(b) T=600 K

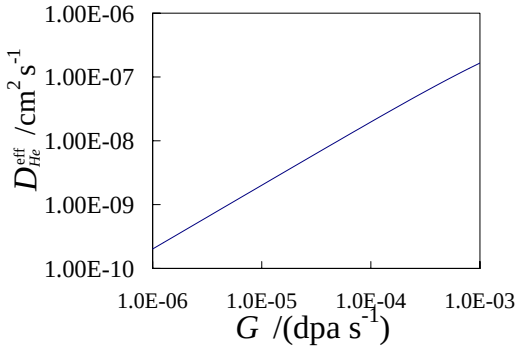

(c) T=800 K

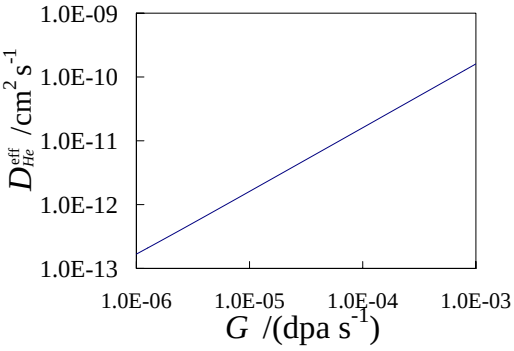

(d) T=1000 K

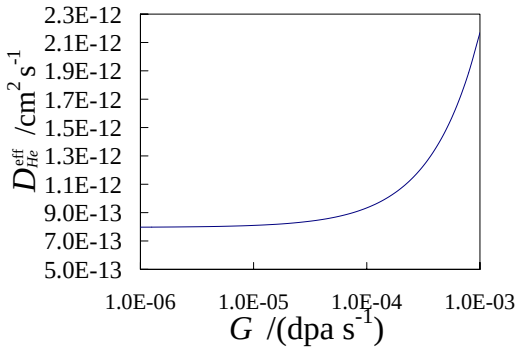

(e) T=1200 K

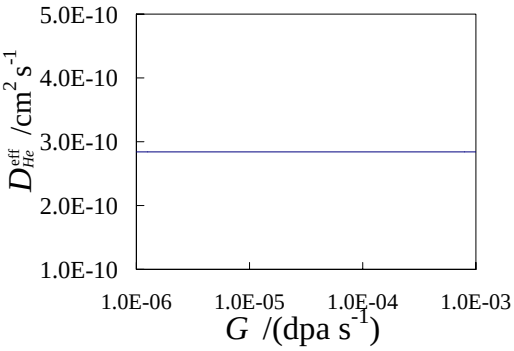

(f) T=1600 K

Figure 3.6: Effective coefficients of helium atoms as a function of radiation damage rates at different temperatures

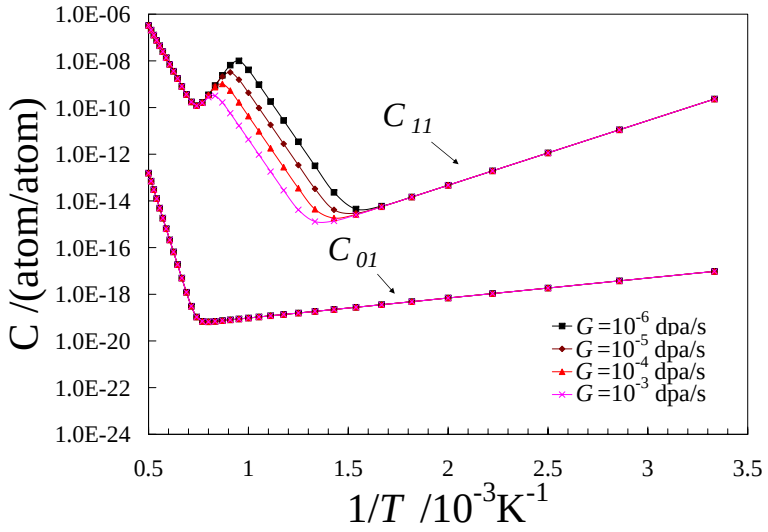

Figure 3.7: Steady state concentrations of the interstitial helium atoms C_{01} and the substitutional helium atoms C_{11} as a function of temperature at different radiation damage rates

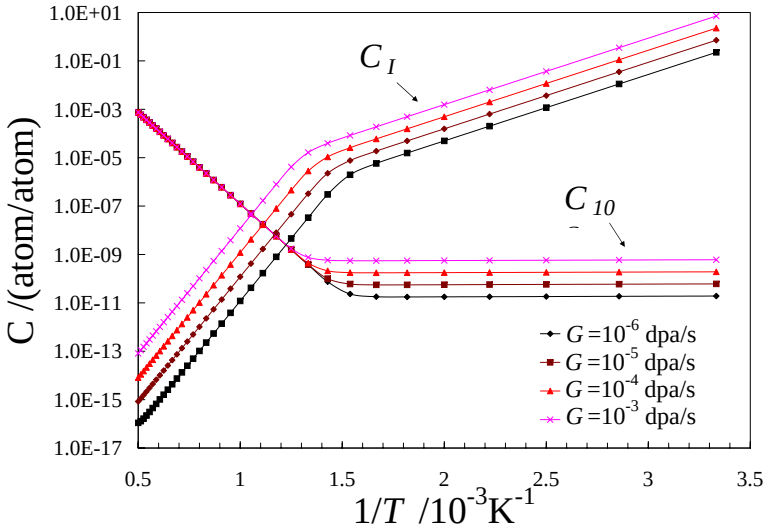

Figure 3.8: Steady state concentrations of the unoccupied vacancies C_{10} and the SIAs C_I as a function of temperature at different radiation damage rates

The effect can be explained by Fig. 3.7 which shows the effect of different radiation damage rates on the steady state concentrations of the interstitial helium atoms C_{01} and the substitutional helium atoms C_{11}. Referring to eqn. (3.2), the enhancement of D_{He}^{eff} is clearly due to the reduction of C_{11} as G increases. Fig. 3.8 shows the effect of different radiation damage rates on the steady state concentrations of the unoccupied vacancies C_{10} and the SIAs C_I, which can justify the effect of G on C_{11} in mechanisms. As discussed in section 3.1, C_{11} is determined by:

$$C_{11} = \frac{R_{10,01} C_{10} C_{01}}{E_{11}^{He}} \tag{3.3}$$

where E_{11}^{He} indicates the dissociation process is dominated by the thermal emission. Since no terms on the left side of the above equation be affected by G at high temperatures, above 1200 K, G has no effect on C_{11}. When the temperature is below 1200 K, C_{11} is determined by:

$$C_{11} = \frac{R_{10,01} C_{10} C_{01}}{R_{I,11} C_I} \tag{3.4}$$

where E_{11}^{He} indicates the dissociation process is dominated by the replacement of SIAs. when $T < 600$ K, the effect of G on both C_I and C_{10} are the same because at this low temperatures, the vacancies and SIAs induced by radiation damage outnumber those induced by thermal activation. They offset each other so that G has no effect on C_{11}. Only when 1200 K $> T >$ 600 K, thermal vacancies are comparable with radiation induced vacancies, does G have its effect on C_{11} via eqn. (3.4). In conclusion, the effect of the radiation damage rate G on the effective diffusion coefficient of helium atoms D_{He}^{eff} arises from the combination of both the dissociation mechanism dominated by the replacement of SIAs and the difference in mechanisms by which vacancies and SIAs are produced.

3.3.2 Effect of helium production rate

The effect of helium production rates G_{He} on the effective diffusion coefficient has also been studied. Fig. 3.9 has shown the effective diffusion coefficient of he-

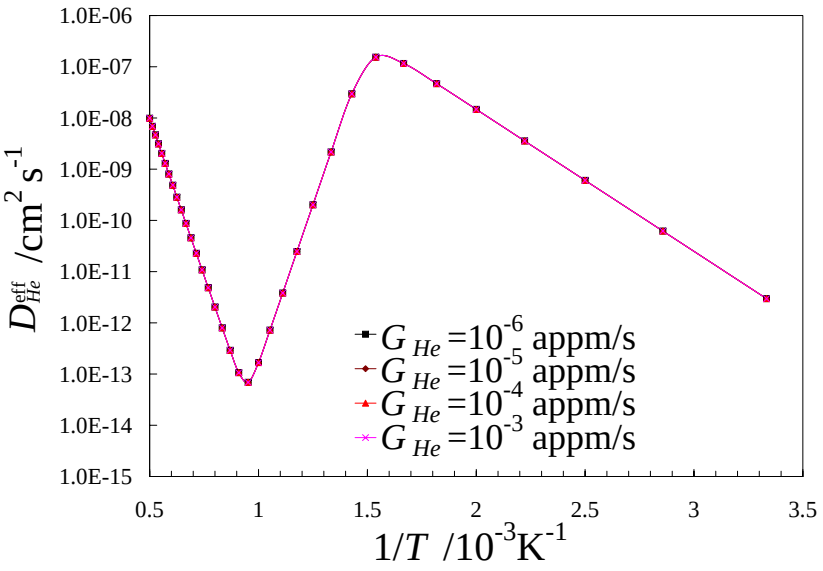

Figure 3.9: Effective diffusion coefficient of helium atoms as a function of temperature

lium atoms D_{He}^{eff} varying with temperatures at different helium production rates. It is found that D_{He}^{eff} is independent on the magnitude of G_{He}. This can be explained by Fig. 3.10 in which the concentrations that determine D_{He}^{eff} were plotted at different helium production rates. Not surprisingly, G_{He} will significantly change the concentrations of helium atoms C_{01} and C_{11} except at very high temperatures. However, the ratios of the two concentrations $f_{01} = \frac{C_{01}}{C_{01}+C_{11}}$, $f_{11} = \frac{C_{11}}{C_{01}+C_{11}}$ are not affected by G_{He}, as shown in Fig. 3.11. Therefore, helium production rates have no effect on the effective diffusion coefficient according to eqn. (2.5). The possibility arises therefore that the helium diffusion data available for materials used in the fission nuclear reactor can also be utilized for the design of materials in the fusion nuclear reactor, since the major difference between those two scenarios is that the latter is characterized by a much larger helium production rate in the surrounding materials [6].

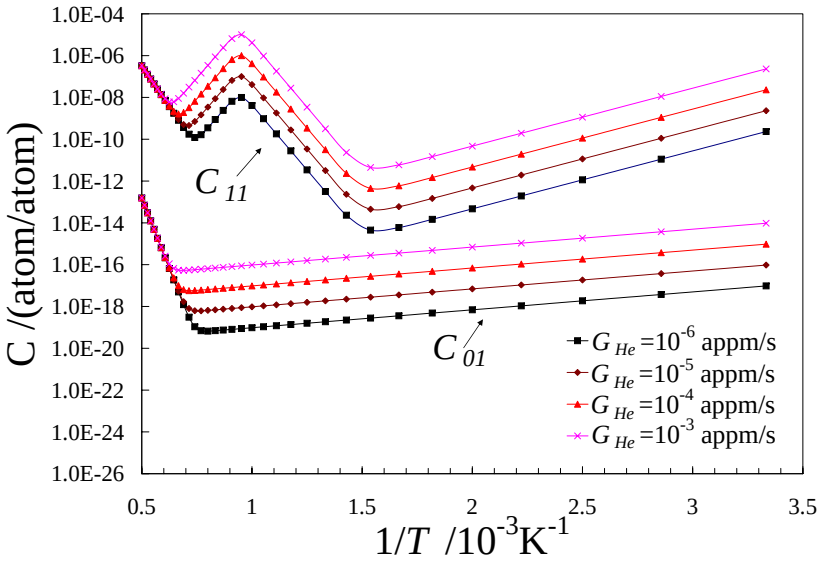

Figure 3.10: Steady state concentrations of the interstitial helium atoms C_{01} and the substitutional helium atoms C_{11} as a function of the helium production rates

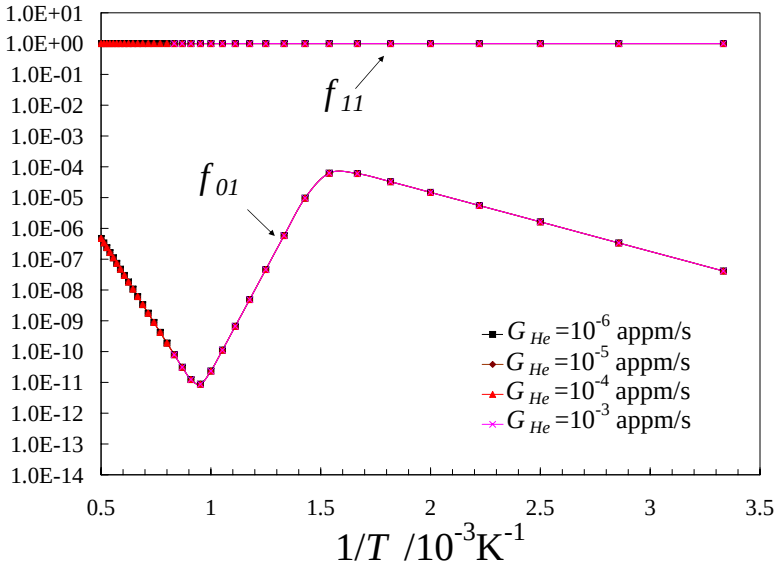

Figure 3.11: Ratios of C_{01} and C_{11} to the total concentration of helium atoms as a function of the helium production rates

3.4 Effect of microstructure on D_{He}^{eff}

Microstructure is thought to have an effect on the diffusion of helium atoms. Cavities, dislocations and grain boundaries act as sinks and annihilate points defects inside the lattice such as vacancies and self-interstitial atoms. Their effects are investigated here by incorporating the parameter of the annihilation probability P^k in the model, as explained in section 2.3.

3.4.1 Effect of cavities

Fig. 3.12 shows the effective diffusion coefficient of helium atoms D_{He}^{eff} varying with temperatures at different configurations of cavities characterized by the radius R_v and the number density N_v. According to eqn. (2.22), the larger N_v and R_v are, the higher the magnitude of P^v is, the more point defects will be annihilated in cavities. Fig. 3.12 shows that the effect of different cavity configurations appears to be really small. Fig. 3.13 shows D_{He}^{eff} varying with R_v at different temperatures. Again, the scale of y-axis implies the small effect of cavities at the temperature range 600 K $\sim$ 1000 K. The reason that D_{He}^{eff} slightly decreases with an increasing N_v and R_v may be explained by the weakening of the dissociation mechanism of helium atoms induced by the replacement of SIAs as more SIAs are annihilated by the cavities.

3.4.2 Effect of dislocations and grain boundaries

Dislocations and grain boundaries are treated differently from cavities in this model as it is believed that the helium atoms trapped in them will diffuse more rapidly than in the perfect lattice. However, dislocation and boundaries still act as sinks for vacancies and SIAs which will be annihilated if they jump into these sinks. Their effects as sinks on the effective diffusion coefficient of helium atoms D_{He}^{eff} are shown in the Fig. 3.14. It can be seen that as sinks, grain boundaries and dislocations have the similar but more significant effect on D_{He}^{eff} compared with

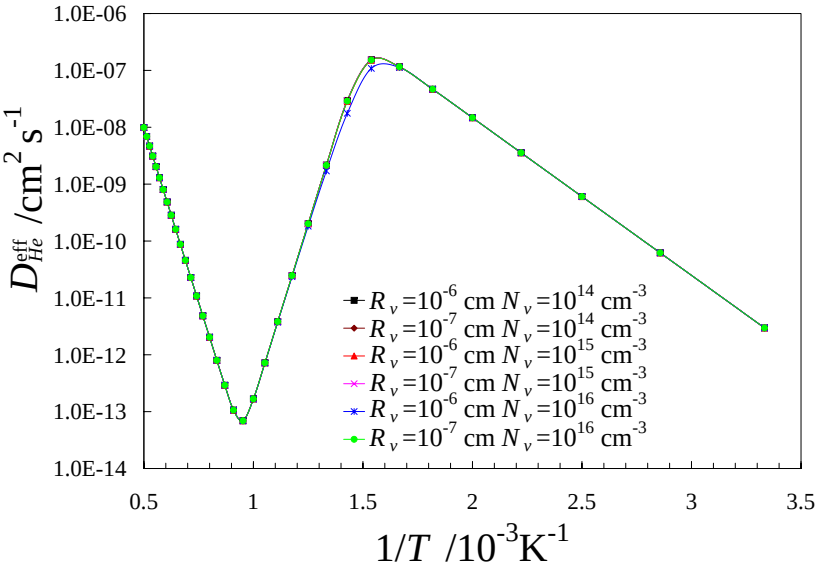

Figure 3.12: Effective diffusion coefficient of helium atoms as a function of temperature

cavities.

On the other hand, the effect of dislocations and grain boundaries as the channel for the pipe diffusion of helium atoms are investigated by using the following equation [23]:

$$D_{He}^{tot} = D_{He}^{\text{eff}} + \frac{\delta}{2R_g} D_{He}^{gb} + (1 - x_d) D_{He}^{d} \tag{3.5}$$

where D^{gb} and D_{He}^{d} are the diffusion coefficients of helium atoms in grain boundaries and dislocations respectively. They can be calculated using:

$$D_{He}^{gb(dl)} = \frac{\lambda^2 \nu_{He}^{o}}{6} \exp\{-E_{He}^{gb(dl)}/kT\} \tag{3.6}$$

where $E_{He}^{gb(dl)}$ the migration energy of helium atom in grain boundaries (dislocations). It is assumed that helium atoms can diffuse interstitially in the grain boundaries (dislocations) so that $E_{He}^{gb(dl)}$ is equal to the interstitial migration energy, E_{He}^{M} *i.e.* 0.17 eV.

δ is the average width of grain boundaries and normally equal to two or three

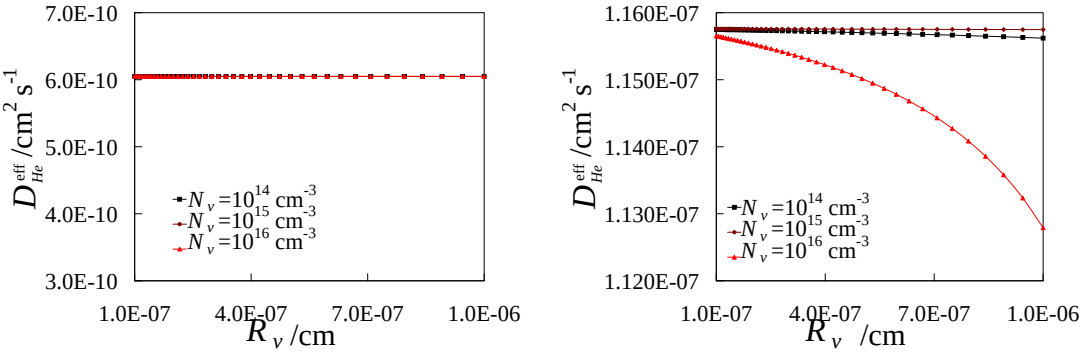

(a) T=400 K

(b) T=600 K

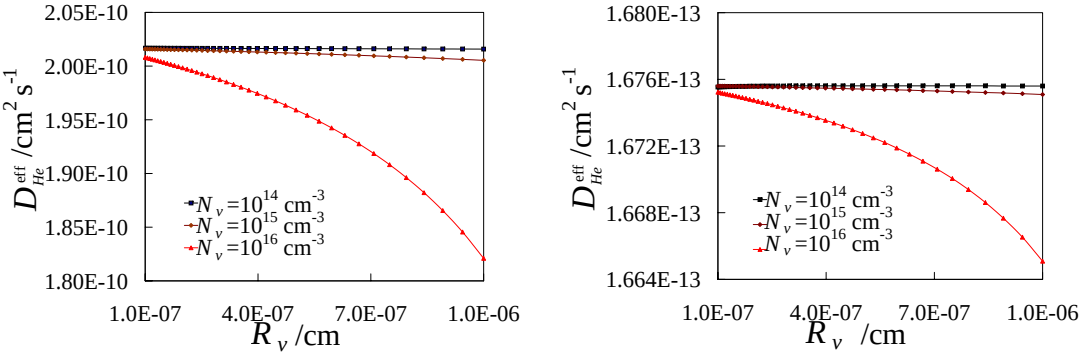

(c) T=800 K

(d) T=1000 K

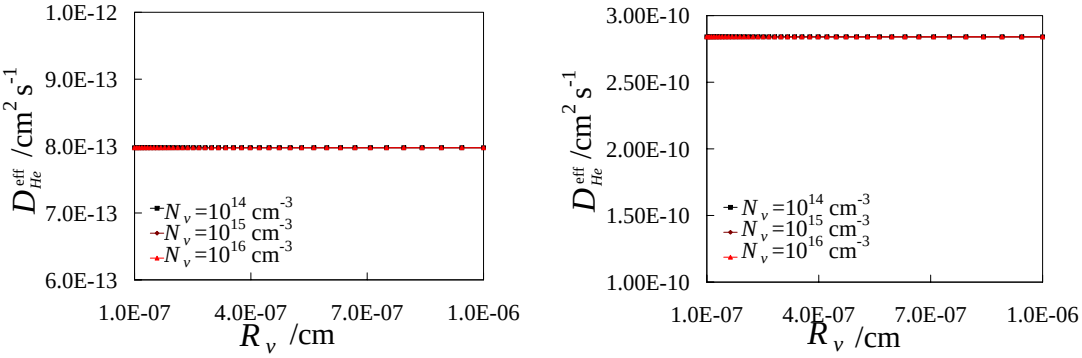

(e) T=1200 K

(f) T=1600 K

Figure 3.13: Effective diffusion coefficient of helium atoms as a function of the average cavity radius at different temperatures

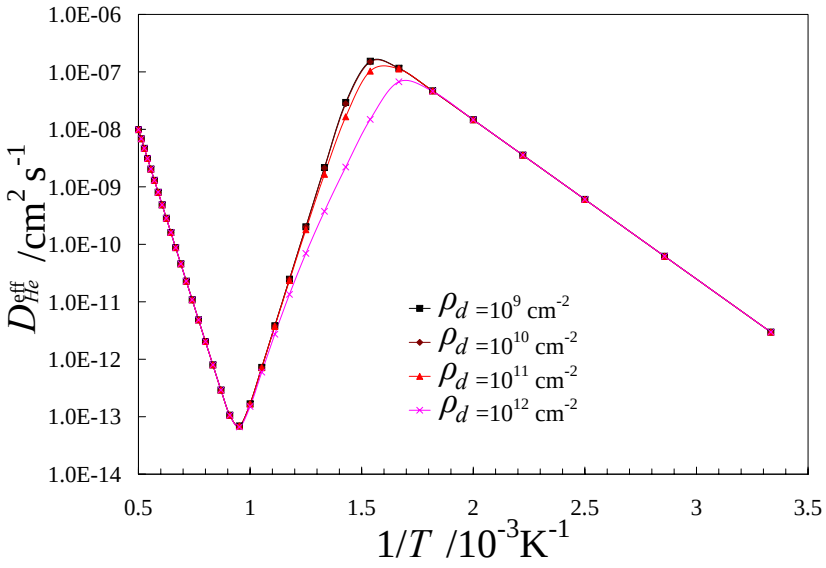

(a)

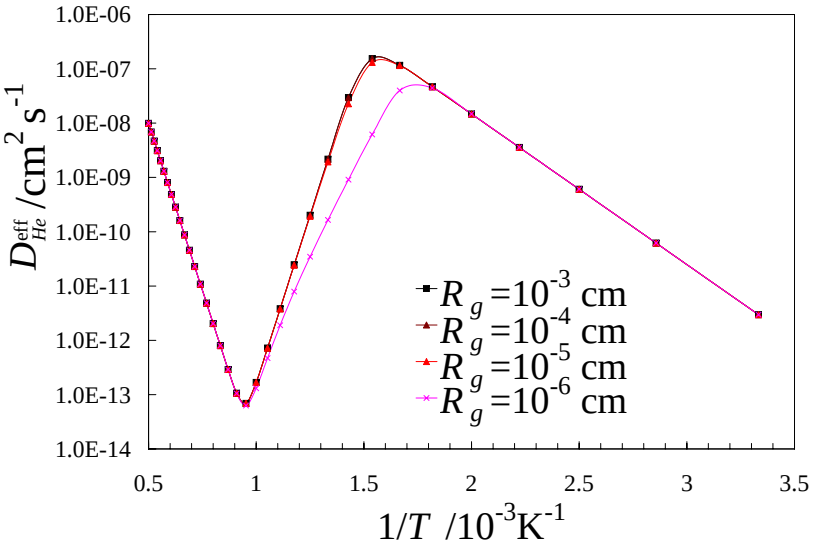

(b)

Figure 3.14: Effective diffusion coefficient of helium atoms as a function of temperature

atoms diameters [23]. x_d is the fractional concentration of atoms in dislocations core region and can be estimated using:

$$x_d = \rho_d \pi r_o^2 \tag{3.7}$$

where ρ_d is the dislocation density and r_o is the radius of metal atoms.
Based on eqn. (3.5–3.7), the analysis of the structure sensitive diffusion of helium atoms can be achieved, as shown in Fig. 3.15.
The solid line in the figure represents D_{He}^{eff} *i.e.* without any dislocations and grain boundaries. The dashed line shows D_{He}^{tot} when the diffusion of helium atoms in dislocations and grain boundaries are taken into account. Fig. 3.15(a) and Fig. 3.15(a) include the dislocation density of 10^{10} cm^{-2}and the average grain radius of 10^{-4} cm respectively. The results indicate both D_{He}^{gb} and D_{He}^{dl} contribute significantly to D_{He}^{eff}, even at high temperatures. This is different from normal dislocation and grain boundary diffusion mechanism whose contribution is negligible compared with the diffusion in the bulk unless at very low temperatures. It is because D_{He}^{eff} in the bulk is given by $\frac{D_{01}C_{01}}{C_{11}}$ where D_{01} is equal to $D_{He}^{dl(gb)}$ as the activation energy for helium atoms migrating interstitially in the bulk E_{He}^{I} is assumed to be same as that in the dislocations (grain boundaries) $E_{He}^{dl(gb)}$, so that the contribution from the bulk $\frac{C_{01}}{C_{11}}$ is comparable to that from the dislocations $(1 - x_d)$ or from the grain boundaries $\frac{\delta}{2R_g}$.
However, it should be pointed out the assumption that helium atoms migrate interstitially in dislocations and grain boundaries without any trapping is simplistic. A more accurate migration energy $E_{He}^{dl(gb)}$ is required in order to use eqn. (3.5) to explain the effect of dislocation (grain boundaries) on the helium diffusion.

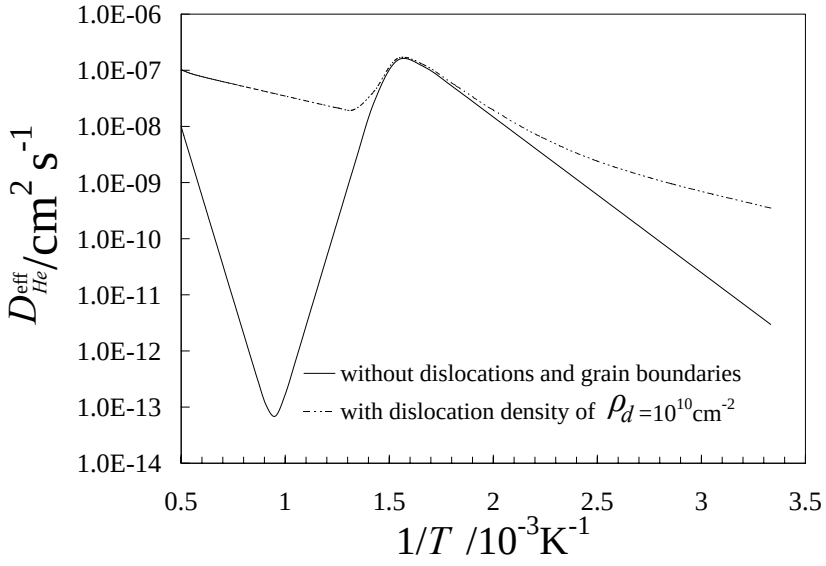

(a)

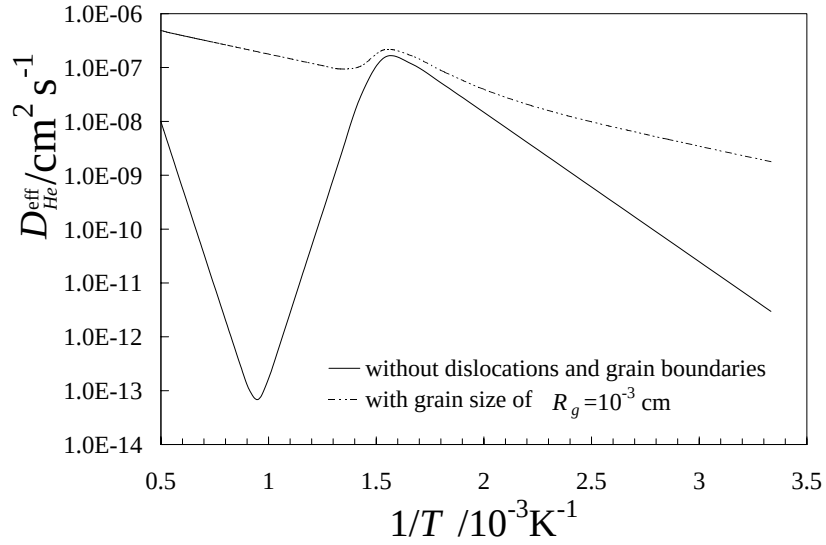

(b)

Figure 3.15: Comparison of helium diffusion with and without the consideration of dislocations and grain boundaries as easy diffusion channels.

Chapter 4

Summary and Conclusions

This chapter summarizes the outcomes of the project, based on which major conclusions are drawn. Future work is suggested.

By calculating the effective diffusion coefficient of helium atoms with rate theory equations, it has been possible to develop a theoretical model of mechanisms by which helium atoms migrate in BCC irons under the irradiation conditions. The model has also been applied to the FCC structure material nickel so that different behaviours of helium diffusion in FCC and BCC can be identified. Particular interests are in explaining the diffusion in BCC iron. It is hoped that the behaviour of the helium diffusion can help to explain the delay of swelling in BCC iron under irradiation. The effects of temperature, helium production rate, radiation damage rate have been investigated. Point defects sinks were also included in the model and their effects have been studied. Major conclusions are:

- Temperature is the predominant factor that determines the mechanism of helium migration. Most of helium atoms stay in the substitutional positions at the steady state and jump from one vacancy to another. At high temperature $T > 1200$ K the detrapping process is dominated by the thermal emission. When 600 K $< T <$ 1200 K , the detrapping process is dominated by the replacement of self-interstitial atoms.

- The effective diffusion coefficient of helium atoms D_{He}^{eff} in BCC is significantly different from that in FCC due to the difference in the detrapping energy E_{He}^{D} and the migration energy of vacancies E_{V}^{M}. The large E_{He}^{D} and small E_{V}^{M} in BCC irons leads to a negative effective diffusion energy at around 600 K–1000 K and relatively large D_{He}^{eff} below 600 K. It may suggest that a larger number density of vacancy-helium clusters and bubbles exists in BCC iron under irradiation which may suppress the swelling.

- Helium production rates have no effect on the effective helium diffusion coefficient because they change the concentrations of helium interstitials atoms and helium substitutional atoms, but not the ratio between them. Radiation damage rates can affect the effective helium diffusion coefficient significantly at medium temperatures between 600 K and 1200 K. It is due to the dissociation mechanism dominated by the replacement of SIAs and the difference in mechanisms by which vacancies and SIAs are produced.

- Point defect sinks such as cavities, grain boundaries and dislocations have effects on D_{He}^{eff}. However, the latter two will affect D_{He}^{eff} significantly if the pipe diffusion of helium atoms are taken into consideration.

Some future work is suggested:

- It is necessary that the model should be validated by experiments in fusion reactors which currently is not available. Hopefully, the validated model can be used to examine the consequences of the helium diffusion on the coalescence and growth of helium bubbles.

- More mobile helium-vacancy complexes C_{ij} should be included in the rate theory equations. A study of the helium diffusion mechanisms at non-steady state will complete the whole model and is helpful to understand the fate of helium atoms in the irradiated materials.

Bibliography

[1] Rothaut J. H., Schroeder H. and Ullmaier H., *Philosophical Magazine A*, **47**:781-795, 1983

[2] Ullmaier H., *Landolt-Bõrnstein New Series III*, **25**:389-435, 1991

[3] Ullmaier H., *Nuclear Fusion*, **24**:1039-1083, 1984

[4] Farrell K., *Effect of Defects in Solids*, **53**:175, 1980

[5] Chernov I. I., Kalashnikov A. N., Kalin B. A. and Binyukova S. Y., *Journal of Nuclear Materials*, **323**:341-345, 2003

[6] Mansur L. K., *Journal of Nuclear Materials*, **216**:97-123, 1994

[7] Braski D. N., Schroeder H. and Ullmaier H., *Journal of Nuclear Materials*, **83**:265-277, 1979

[8] Gelles D. S., *Journal of Nuclear Materials*, **283-287**:838-840, 2000

[9] Bloom E. E., *Journal of Nuclear Materials*, **85-86**:795-804, 1979

[10] Byun T. S. and Farrell K., *Journal of Nuclear Materials*, **329-333**:998-1002, 2004

[11] Ullmaier H. and Chen J., *Journal of Nuclear Materials*, **318**:228-233, 2003

[12] Philipps V., Sonnenberg K. and Williams J. M., *Journal of Nuclear Materials*,**114**:95-97, 1983

[13] Philipps V. and Sonnenberg K., *Journal of Nuclear Materials*, **107**:271-279, 1982

[14] Poker D. B. and Williams J. M., *Applied Physics Letters*, **40**:851-852, 1982

[15] Reed D. J., *Radiation Effects*, **31**:129-147, 1977

[16] Trinkaus H. and Singh B. N., *Journal of Nuclear Materials*, **323**:229-242, 2003

[17] Trinkaus H., *Journal of Nuclear Materials*, **118**:39-49, 1983

[18] Foreman A. J. E and Singh B. N., *Journal of Nuclear Materials*, **141-143**:672-676, 1986

[19] Ghoniem N. M., Sharafat S., Williams J.M. and Mansur L.K., *Journal of Nuclear Materials*, **117**:96-105, 1983

[20] Wilson W. D. and Johnson R. A., *Interatomic Potentials and simulation of Lattice Defects*, edited by Gehlen C., Beeler J. R. and Jaffee R. I. (Plenum, New York 1972) p. 375

[21] Singh B.N., Foreman A.J.E., *Journal of Nuclear Materials*, **122-123**:537-541, 1984

[22] Russell K. C., *Acta Metallurgica*, **26**:1615-1630, 1978

[23] Christian J. W., *the Theory of Transformation in Metals and Alloys (second edition)*, edited by Christian J. W., (Pergamon Press Ltd, Oxford, 1975)

[24] Ghoniem N. M., Takata M. L., *Journal of Nuclear Materials*, **105**:276-292, 1982

[25] Olander D. R., *Fundamental Aspects of Nuclear Reactor Fuel Elements*, **TID-26711-P1** (NTIS, Springfield, VA, 1976)

[26] Loh B. T. M., *Acta Metallurgica*, **20**:1305, 1972

[27] Ghoniem N. M. and Cho D. D., *Physica Status Solidi*, **54**:171, 1979

[28] Wolfer W. G. and Ashkin M., *Journal of Applied Physics*, **46**:547, 1975

[29] Kornelsen E. V. and Van Gorkum A. A., *Journal of Nuclear Materials*, **92**:79, 1980

[30] Wiedersich H., *Radiation Effects*, **12**:111-125, 1972

[31] Radhakrishnan K. and Hindmarsh A. C., *LLNL report UCRL-ID-113855*, http://www.llnl.gov/CASC/nsde/pubs/u113855.pdf, 1993

[32] Braisford A. D. and Bullough R., *Philosophical Transactions of the Royal Society of London. Series A, Mathematical and Physical Sciences*, **302**:87-137, 1981

[33] Johnson R. A., *Physics Review*, **145**:423, 1966

[34] Ghoniem N. M. and Conn R. W., *Process LAEA Technical Committee Meeting*, Oct. 1981, Tokyo, Japan

[35] Seeger A., and Mehrer H., *Vacancies and Interstitials in Metals*, edited by Seeger A., Schumacher, Schilling W. and Diehl J. (North-Holland, Amsterdam, 1970), p. 1

[36] Wiedersich H., Burton J.J. and Katz J.L., *Journal of Nuclear Materials*, **51**:287-301, 1974

[37] Kemp R., Sonny M., Jacob T., Chen J., Zhang Y., Bhadeshia, H. K. D. H., http://www.msm.cam.ac.uk/map/steel/programs/irradiated.austenitic.html

[38] Morishita K., Sugano R., Wirth B. D., *Fusion science and technology*, **44**:441-445, 2003

Appendix A

FORTRAN Program

HELIUM_DIFFUSION

This appendix presents the model described in Chapter 2 and associated documentation following the MAP format,
http://www.msm.cam.ac.uk/map/mapmain.html.

Provenance of Source Code

Yucheng Zhang
Phase Transformations and Complex Properties Group,
Department of Materials Science and Metallurgy,
University of Cambridge, CB2 3QZ,
United Kingdom.

This program uses DLSODE subroutine to solve ordinary differential equations. The subroutine is presented by:
Lawrence Livermore National Laboratory
Livermore, CA 94551, U.S.A.
It is downloadable on http://www.llnl.gov/CASC/odepack.

Purpose

A program to calculate the effective diffusion coefficient of helium atoms in irradiated materials as a function of temperature, radiation damage rate, helium production rate and microstucture.

Specification

Language: FORTRAN
Product Form: Source Code
Operating System: tested on Linux

Description

HELIUM_DIFFUSION contains the program which enables the user to calculate the effective diffusion coefficient of helium atoms in irradiated materials as a function of temperature, radiation damage rate, helium production rate, microstucture parameters including dislocation density, average grain size, average size and number density of cavities. Once uncompressed, HELIUM_DIFFUSION contains:

HELIUM_DIFFUSION_BCC.f
The source code to calculate the helium diffusion in BCC iron.

heliums_DIFFUSION_FCC.f
The source code to calculate the helium diffusion in FCC nickel.

BCC
The executable file of heliums_DIFFUSION_BCC.f

FCC
The executable file of heliums_DIFFUSION_FCC.f

input.txt
The input file

output_bcc.txt
The output file for BCC

output_fcc.txt
The output file for FCC

Readme.txt
A text file containing instructions for compiling and running the program.

Reference

1. Yucheng Zhang, Master of philosophy (M.Phil) thesis, Chapter 2, University of Cambridge, 2003

2. [31]

Input Parameters

The user is required to provide:
the temperature T - the radiation damage rate G - the helium production rate G_{He} - the dislocation density ρ_d - the average radius of grains R_g - the average radius of cavities R_v - the number density of cavities N_v.

Output Parameters

The default outputs are:
The reciprocal of the temperature T - the concentration of vacancies C_{10} - the concentration of SIAs C_I - the concentration of interstitial helium atoms C_{01} - the concentration of substitutional helium atoms C_{11} - the diffusion coefficient of helium atoms migrating interstitially D_{01} - the diffusion coefficient of helium atoms migrating substitutionally D_{11} - the effective diffusion coefficient D_{He}^{eff} - the total diffusion coefficient D_{He}^{tot}.

Keywords
helium diffusion, effective diffusion coefficient, BCC iron, irradiation

Example

I. Program test

Complete program

II. Input

In the file input, an example is as follows:

```
300D0   1.00D-6   1.00D-6   0.00D+9   0.00D-4   1.00D-6   1.00D14
350D0   1.00D-6   1.00D-6   0.00D+9   0.00D-4   1.00D-6   1.00D14
400D0   1.00D-6   1.00D-6   0.00D+9   0.00D-4   1.00D-6   1.00D14
450D0   1.00D-6   1.00D-6   0.00D+9   0.00D-4   1.00D-6   1.00D14
500D0   1.00D-6   1.00D-6   0.00D+9   0.00D-4   1.00D-6   1.00D14
600D0   1.00D-6   1.00D-6   0.00D+9   0.00D-4   1.00D-6   1.00D14
650D0   1.00D-6   1.00D-6   0.00D+9   0.00D-4   1.00D-6   1.00D14
700D0   1.00D-6   1.00D-6   0.00D+9   0.00D-4   1.00D-6   1.00D14
750D0   1.00D-6   1.00D-6   0.00D+9   0.00D-4   1.00D-6   1.00D14
800D0   1.00D-6   1.00D-6   0.00D+9   0.00D-4   1.00D-6   1.00D14
```

```
 850D0   1.00D-6   1.00D-6   0.00D+9   0.00D-4   1.00D-6   1.00D14
 900D0   1.00D-6   1.00D-6   0.00D+9   0.00D-4   1.00D-6   1.00D14
 950D0   1.00D-6   1.00D-6   0.00D+9   0.00D-4   1.00D-6   1.00D14
1000D0   1.00D-6   1.00D-6   0.00D+9   0.00D-4   1.00D-6   1.00D14
1050D0   1.00D-6   1.00D-6   0.00D+9   0.00D-4   1.00D-6   1.00D14
1100D0   1.00D-6   1.00D-6   0.00D+9   0.00D-4   1.00D-6   1.00D14
1150D0   1.00D-6   1.00D-6   0.00D+9   0.00D-4   1.00D-6   1.00D14
1200D0   1.00D-6   1.00D-6   0.00D+9   0.00D-4   1.00D-6   1.00D14
1250D0   1.00D-6   1.00D-6   0.00D+9   0.00D-4   1.00D-6   1.00D14
1300D0   1.00D-6   1.00D-6   0.00D+9   0.00D-4   1.00D-6   1.00D14
1350D0   1.00D-6   1.00D-6   0.00D+9   0.00D-4   1.00D-6   1.00D14
1400D0   1.00D-6   1.00D-6   0.00D+9   0.00D-4   1.00D-6   1.00D14
1450D0   1.00D-6   1.00D-6   0.00D+9   0.00D-4   1.00D-6   1.00D14
1500D0   1.00D-6   1.00D-6   0.00D+9   0.00D-4   1.00D-6   1.00D14
1550D0   1.00D-6   1.00D-6   0.00D+9   0.00D-4   1.00D-6   1.00D14
1600D0   1.00D-6   1.00D-6   0.00D+9   0.00D-4   1.00D-6   1.00D14
1650D0   1.00D-6   1.00D-6   0.00D+9   0.00D-4   1.00D-6   1.00D14
1700D0   1.00D-6   1.00D-6   0.00D+9   0.00D-4   1.00D-6   1.00D14
1750D0   1.00D-6   1.00D-6   0.00D+9   0.00D-4   1.00D-6   1.00D14
1800D0   1.00D-6   1.00D-6   0.00D+9   0.00D-4   1.00D-6   1.00D14
1850D0   1.00D-6   1.00D-6   0.00D+9   0.00D-4   1.00D-6   1.00D14
1900D0   1.00D-6   1.00D-6   0.00D+9   0.00D-4   1.00D-6   1.00D14
1950D0   1.00D-6   1.00D-6   0.00D+9   0.00D-4   1.00D-6   1.00D14
2000D0   1.00D-6   1.00D-6   0.00D+9   0.00D-4   1.00D-6   1.00D14
```

III. Output

In the file output we obtain the following results:

```
3.3333  0.191853E-10  0.226423E+00  0.960081E-17  0.232420E-09
0.100157E-59  0.717231E-04  0.296274E-11  0.296274E-11
2.8571  0.186625E-10  0.111411E-01  0.375241E-17  0.111245E-10
```

0.260995E-50 0.183509E-03 0.618993E-10 0.618993E-10
2.5000 0.182796E-10 0.116394E-02 0.185486E-17 0.113838E-11
0.301021E-43 0.371240E-03 0.604894E-09 0.604894E-09
2.2222 0.179867E-10 0.200871E-03 0.107229E-17 0.193328E-12
0.935933E-38 0.642176E-03 0.356181E-08 0.356181E-08
2.0000 0.177553E-10 0.492512E-04 0.691694E-18 0.468148E-13
0.231936E-33 0.995527E-03 0.147088E-07 0.147088E-07
1.8182 0.176005E-10 0.155550E-04 0.483207E-18 0.147334E-13
0.912078E-30 0.142506E-02 0.467359E-07 0.467359E-07
1.6667 0.179624E-10 0.578412E-05 0.358357E-18 0.594879E-14
0.886293E-27 0.192155E-02 0.115748E-06 0.115748E-06
1.5385 0.232646E-10 0.196594E-05 0.278272E-18 0.447862E-14
0.254448E-24 0.247455E-02 0.153743E-06 0.153743E-06
1.4286 0.749376E-10 0.303259E-06 0.224035E-18 0.232942E-13
0.172979E-22 0.307362E-02 0.295608E-07 0.295608E-07
1.3333 0.373457E-09 0.332016E-07 0.185659E-18 0.317897E-12
0.451396E-21 0.370894E-02 0.216611E-08 0.216611E-08
1.2500 0.158993E-08 0.458484E-08 0.157513E-18 0.341599E-11
0.761243E-20 0.437169E-02 0.201582E-09 0.201582E-09
1.1765 0.571757E-08 0.797574E-09 0.136244E-18 0.278631E-10
0.919742E-19 0.505416E-02 0.247137E-10 0.247137E-10
1.1111 0.178371E-07 0.168467E-09 0.119762E-18 0.180047E-09
0.842453E-18 0.574975E-02 0.382457E-11 0.382457E-11
1.0526 0.493658E-07 0.419093E-10 0.106712E-18 0.954026E-09
0.611185E-17 0.645288E-02 0.721789E-12 0.721789E-12
1.0000 0.123401E-06 0.119814E-10 0.961875E-19 0.411047E-08
0.363695E-16 0.715893E-02 0.167560E-12 0.167560E-12
0.9524 0.282694E-06 0.385911E-11 0.875627E-19 0.999189E-08
0.182614E-15 0.786408E-02 0.690986E-13 0.690986E-13
0.9091 0.600603E-06 0.137780E-11 0.803962E-19 0.651933E-08

0.791810E-15 0.856523E-02 0.106418E-12 0.106418E-12
0.8696 0.119509E-05 0.537987E-12 0.743802E-19 0.239124E-08
0.302210E-14 0.925986E-02 0.291052E-12 0.291052E-12
0.8333 0.224549E-05 0.227185E-12 0.693878E-19 0.876703E-09
0.103163E-13 0.994598E-02 0.797504E-12 0.797504E-12
0.8000 0.401153E-05 0.102785E-12 0.660509E-19 0.350161E-09
0.319214E-13 0.106220E-01 0.203556E-11 0.203556E-11
0.7692 0.685369E-05 0.494266E-13 0.693036E-19 0.164627E-09
0.905531E-13 0.112868E-01 0.484198E-11 0.484198E-11
0.7407 0.112540E-04 0.250920E-13 0.106474E-18 0.120261E-09
0.237784E-12 0.119393E-01 0.108084E-10 0.108084E-10
0.7143 0.178364E-04 0.133699E-13 0.307714E-18 0.174276E-09
0.582793E-12 0.125790E-01 0.227932E-10 0.227932E-10
0.6897 0.273850E-04 0.743989E-14 0.122285E-17 0.364225E-09
0.134275E-11 0.132054E-01 0.456786E-10 0.456786E-10
0.6667 0.408606E-04 0.430493E-14 0.494160E-17 0.807971E-09
0.292625E-11 0.138181E-01 0.874384E-10 0.874384E-10
0.6452 0.594134E-04 0.258046E-14 0.186866E-16 0.174347E-08
0.606456E-11 0.144169E-01 0.160586E-09 0.160586E-09
0.6250 0.843924E-04 0.159716E-14 0.653680E-16 0.360459E-08
0.120090E-10 0.150019E-01 0.284064E-09 0.284064E-09
0.6061 0.117350E-03 0.101797E-14 0.212219E-15 0.714072E-08
0.228157E-10 0.155731E-01 0.485640E-09 0.485640E-09
0.5882 0.160045E-03 0.666734E-15 0.643073E-15 0.135933E-07
0.417411E-10 0.161305E-01 0.804844E-09 0.804844E-09
0.5714 0.214438E-03 0.448241E-15 0.182920E-14 0.249452E-07
0.737740E-10 0.166743E-01 0.129648E-08 0.129648E-08
0.5556 0.282683E-03 0.309521E-15 0.490969E-14 0.442619E-07
0.126329E-09 0.172047E-01 0.203473E-08 0.203473E-08
0.5405 0.367124E-03 0.220388E-15 0.124931E-13 0.761434E-07

0.210123E-09 0.177219E-01 0.311783E-08 0.311783E-08
0.5263 0.470275E-03 0.163383E-15 0.302650E-13 0.127307E-06
0.340264E-09 0.182263E-01 0.467326E-08 0.467326E-08
0.5128 0.594806E-03 0.128429E-15 0.700657E-13 0.207319E-06
0.537554E-09 0.187181E-01 0.686354E-08 0.686354E-08
0.5000 0.743529E-03 0.109937E-15 0.155540E-12 0.329498E-06
0.830038E-09 0.191976E-01 0.989229E-08 0.989229E-08